Axion-like Particle

At the LHC and HL-LHC

Kingman Cheung, December 2024

Contents

- Motivations for axions
- Summary of current limits on axion or axion-like particle (ALP)
- Use of the ALP to explain excess in $H \to Z\gamma$
- Probing the ALP-gauge couplings

Axion is a strong case of Physics Beyond the SM

- Solve the strong QCD problem
- A potential dark matter candidate
- Unlike SUSY, it does not solve the hierarchy problem.

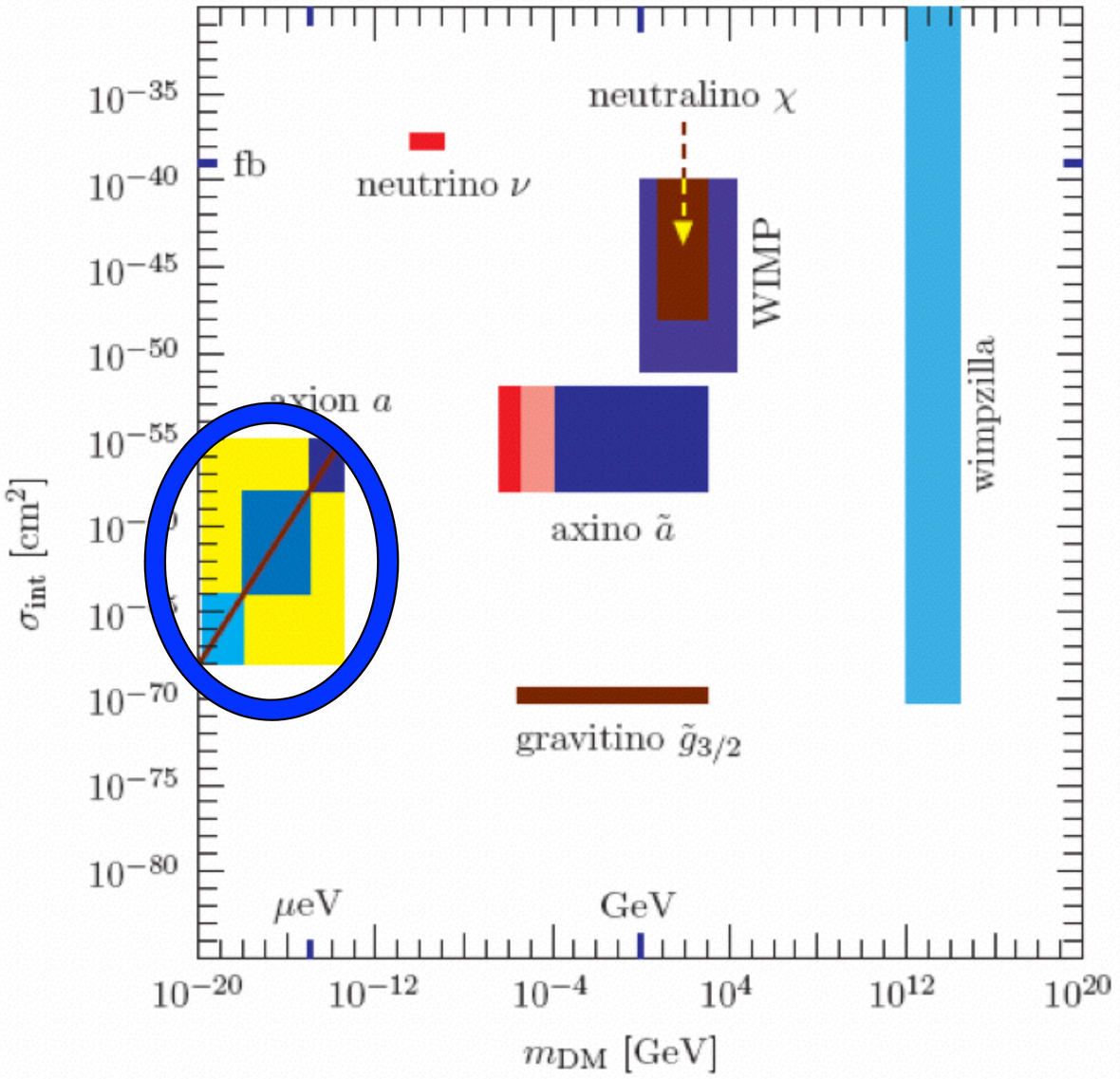

Strong QCD Problem: the θ term in QCD

- QCD Lagrangian: here $-\pi \leq \bar{\theta} \leq \pi$

$$\mathscr{L} = \bar{q}(i\gamma_\mu D^\mu - M_q)q - \frac{1}{4} G^a_{\mu\nu} G^{a,\mu\nu} - \frac{\alpha_s}{8\pi} \bar{\theta}\, G^a_{\mu\nu} \tilde{G}^{a,\mu\nu}$$

- This θ term violates T and P, thus CP.
- Most sensitive probe of T and P violation in flavor-conserving process:

  EDM of neutron

$$d_n(\bar{\theta}) = 2.4 \times 10^{-16}\, \bar{\theta} \;\; e\text{cm}$$

- Experiment: current best limit:

$$|d_n| = (0.0 \pm 1.1_{\text{stat}} \pm 0.2_{\text{sys}}) \times 10^{-26} \;\; e\text{cm}$$ [Abel etal 2020]

- It implies

$$|\bar{\theta}| < 10^{-10}$$

Strong CP problem: why $\bar{\theta}$ is so small.

A Dynamical solution: axion field

- Dynamical solution of strong CP problem based on observation that the vacuum energy in QCD has minimum at $\bar{\theta} = 0$

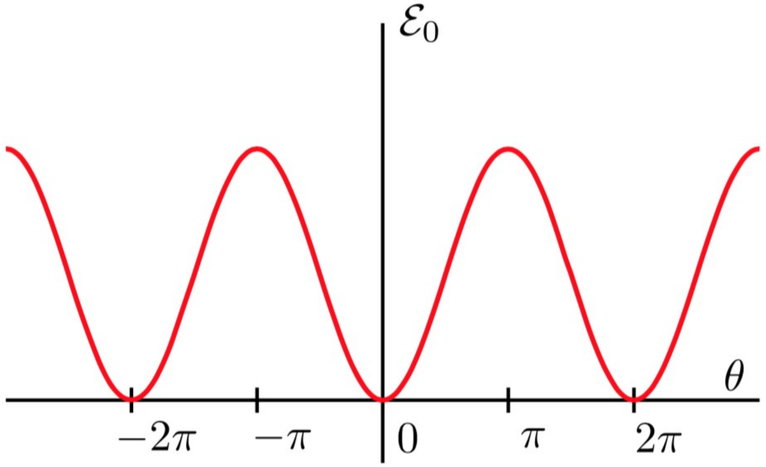

$$\epsilon_0(\bar{\theta}) \simeq \Sigma\ (m_u + m_d)\left(1 - \frac{\sqrt{m_u^2 + m_d^2 + 2m_u m_d \cos\bar{\theta}}}{m_u + m_d}\right)$$

$$\Sigma = -\langle \bar{u}u \rangle = -\langle dd \rangle$$

[Di Vecchia,Veneziano `80; Leutwyler,Smilga 92]

- If $\bar{\theta}$ is a dynamical field, $\bar{\theta}(x) = a(x)/f_a$. Its VEV would be zero (to solve the strong CP)
- The particle excitation is called the axion.
- The mass: $m_a \simeq \frac{\sqrt{\Sigma}}{f_a}\sqrt{\frac{m_u m_d}{m_u + m_d}} \simeq \frac{m_\pi f_\pi}{f_a}\frac{\sqrt{m_u m_d}}{m_u + m_d} \simeq 6\,\mathrm{meV}\left(\frac{10^9\,\mathrm{GeV}}{f_a}\right)$. Note if it is not the QCD axion, this mass relation does not hold.

- Because of CP-odd nature of Axion-like Particle (ALP), it can couplings to gauge bosons:
  1. $\frac{a}{f_a} G^a_{\mu\nu} \tilde{G}^{a\mu\nu}$
  2. $\frac{a}{f_a} B_{\mu\nu} \tilde{B}^{\mu\nu}$
  3. $\frac{a}{f_a} W^i_{\mu\nu} \tilde{W}^{i\mu\nu}$
  4. $\frac{\partial^\mu a}{f_a} \bar{f} \gamma_\mu \gamma_5 f = \frac{a}{f_a} m_a \bar{f} \gamma_5 f$
- Lots of constraints on $g_{a\gamma\gamma}$ from astrophysical and cosmological processes.
- There are also constraints on other ALP-gauge, ALP-top couplings from colliders for Heavier ALP.

Credit: by Ciaran O'hare :: https://cajohare.github.io/AxionLimits/

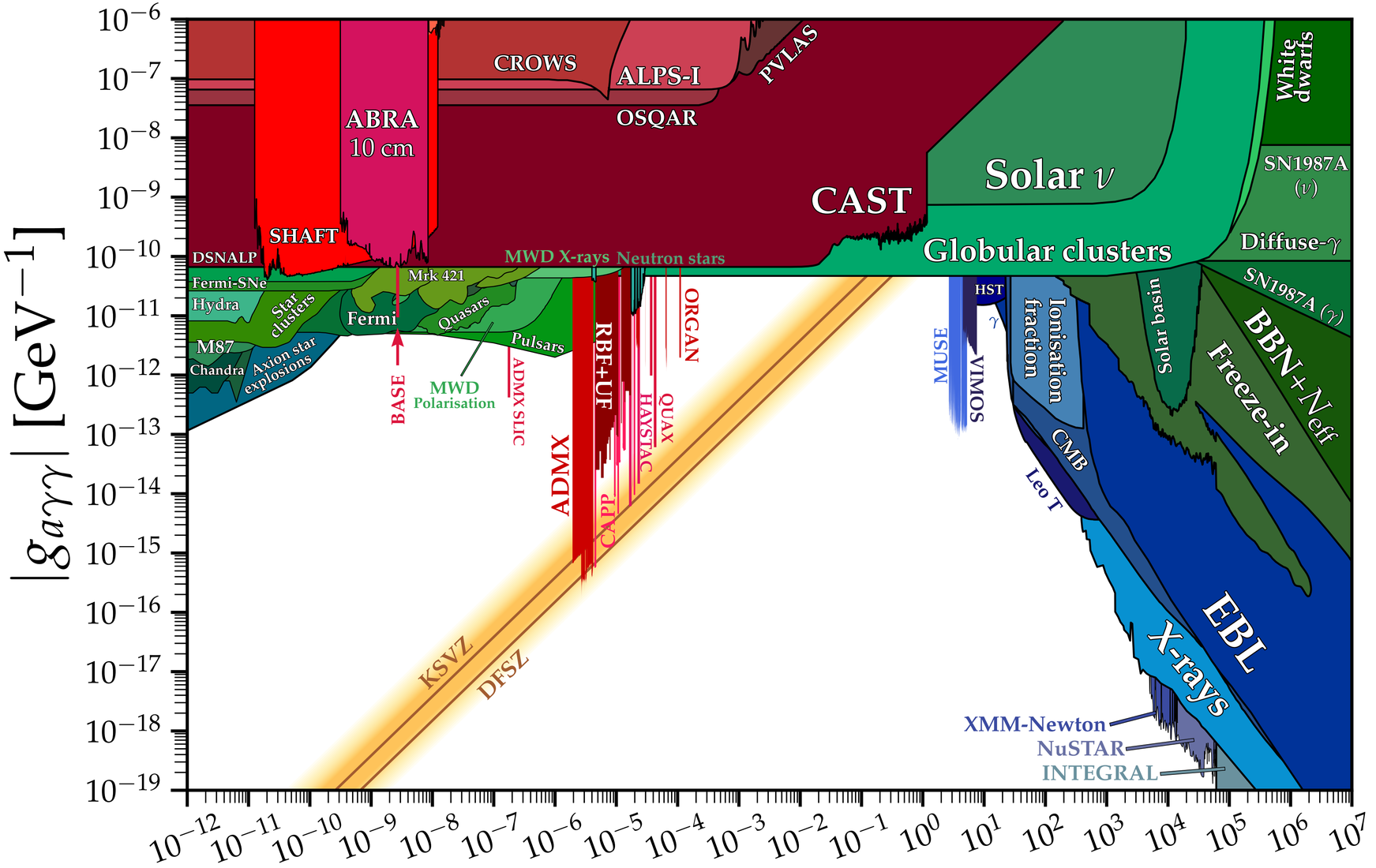

$$\mathscr{L} = -\frac{1}{4} g_{a\gamma\gamma} a F_{\mu\nu} \tilde{F}^{\mu\nu} - \frac{1}{4} g_{aZZ} a Z_{\mu\nu} \tilde{Z}^{\mu\nu} + \ldots$$

Credit: by Ciaran O'hare :: https://cajohare.github.io/AxionLimits/

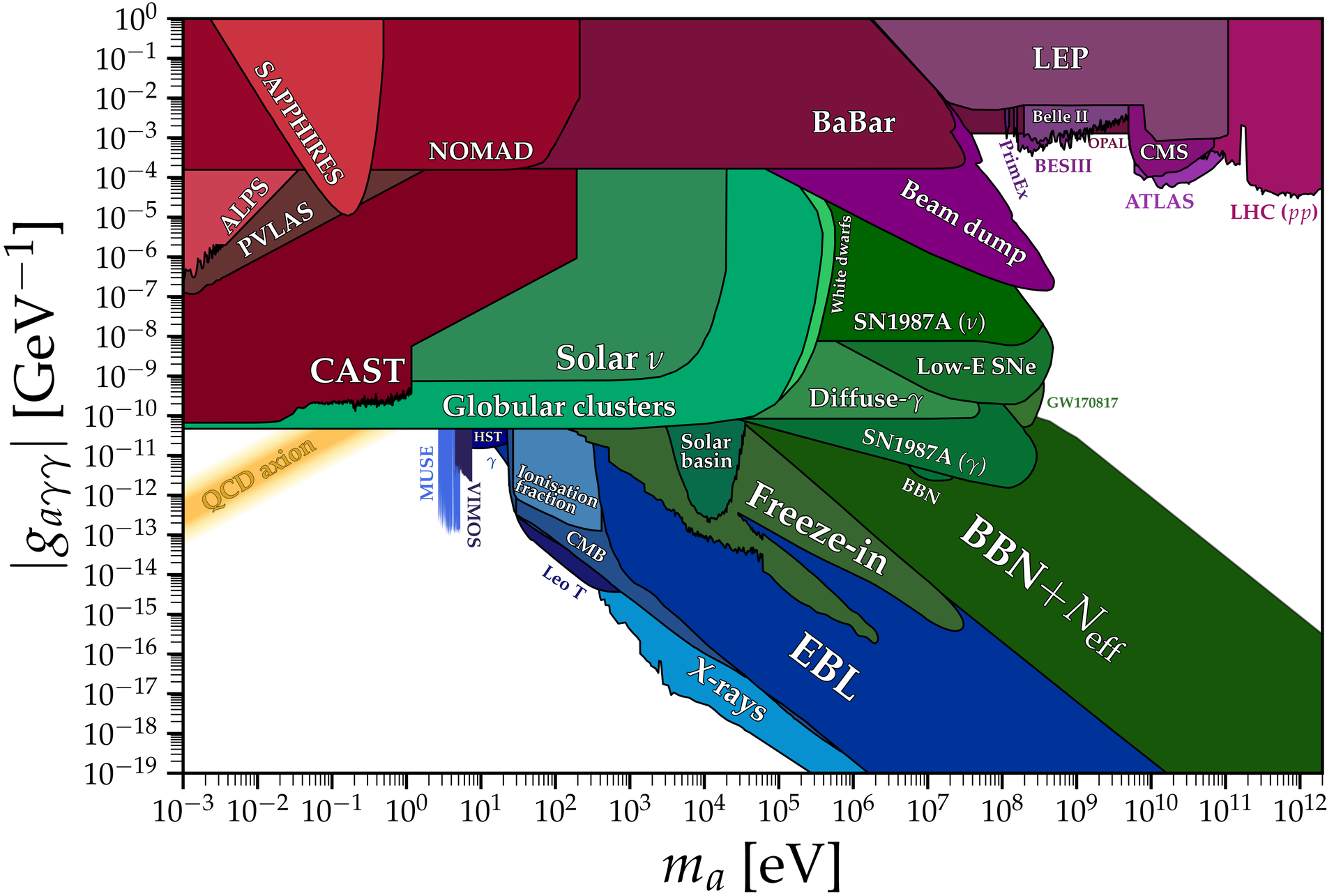

$\sqrt{s} = 250$ GeV with an integrated luminosity 2 ab^{-1},

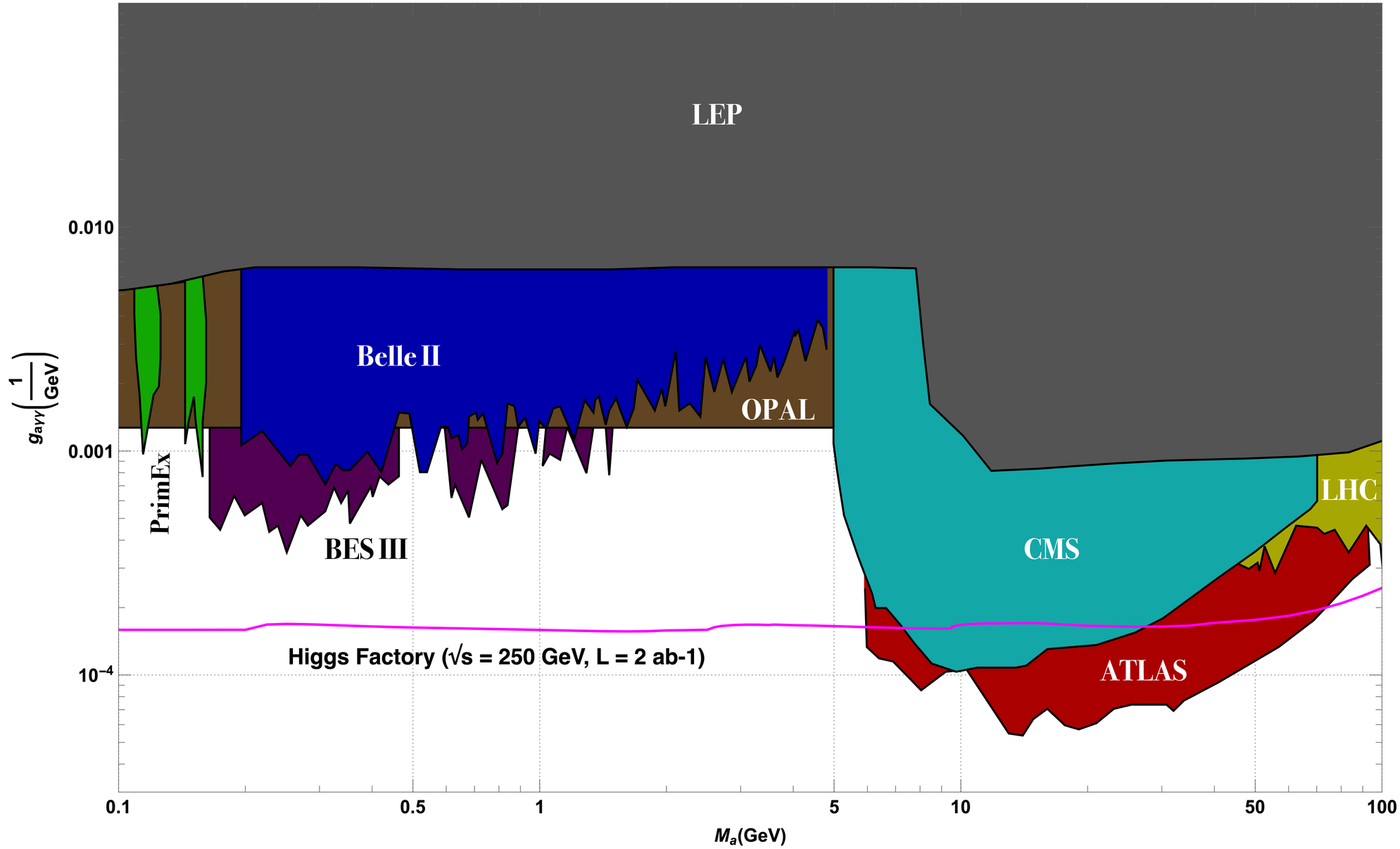

K.C., Ouseph, 2303.16514

References

1. Probing charged lepton flavor violation with axion-like particles at Belle II.
   JHEP 11 (2021) 218.
2. Atmospheric axionlike particles at Super-Kamiokande, Phys.Rev.D 106 (2022) 9, 095029
3. Axionlike particle search at Higgs factories, Phys.Rev.D 108 (2023) 3, 035003
4. Interpretation of excess in $H \to Z\gamma$ using a light axion-like particle, e-Print: 2402.05678,
   PRD in press (discussed today).
5. Probing the gauge-boson couplings of axion-like particle at the LHC and high-luminosity LHC,
   JHEP 05 (2024) 324. (Discussed today)
6. Quark flavor violation and axion-like particles from top-quark decays at the LHC,
   e-Print: 2404.06126 [hep-ph]
7. Exploring interference effects between two ALP effective operators at the LHC,
   e-Print: 2404.14833 [hep-ph]..

Interpretation of excess in $H \to Z\gamma$ by a light ALP

K.C., Ouseph 2402.05678, PRD

Motivation for this work

- Higgs decay $H \to Z\gamma$ is one of the most anticipated modes in future measurements
- The current result from CMS and ATLAS: (showing an excess of 1.9 sigma)

$$B(H \to Z\gamma)_{\text{measured}} = (3.4 \pm 1.1) \times 10^{-3}$$

BUT $$B(H \to Z\gamma)_{\text{sm}} = (1.5 \pm 0.1) \times 10^{-3}$$ (Phys. Rev. Lett. 132 (2024) 021803, [2309.03501].

- This can be explained by putting new particles in the triangular loop, but it needs some fine-tuning so as not to overproduce $H \to \gamma\gamma$.
- We attempt to use the a very light axion-like particle ($m_a < 0.1\,\text{GeV}$), such that when it decays into a collimated photon pair, which looks like a single photon.

- The Higgs boson is mainly produced by gluon fusion, so that Higgs does not have a high p_T
- Taking into account the massive Z boson, the energy of the ALP is

$$p^0(a) \approx \frac{m_H}{2}\left(1 - \frac{m_Z^2}{m_H^2}\right) \approx \frac{m_H}{4}$$

- The opening angle of the photon pair from the ALP decay is

$$\Delta R \sim \frac{2m_a}{p_{T_a}} \approx (3-7) \times 10^{-3}$$

For $m_a = 0.05 - 0.1\,\mathrm{GeV}$

- It is below the angular resolution of the ECAL in CMS and ATLAS. So it appears as a single photon.
- It is smaller than the $\Delta\eta \times \Delta\phi$ of each cell, e.g., ATLAS ECAL: 0.025 x 0.0245.

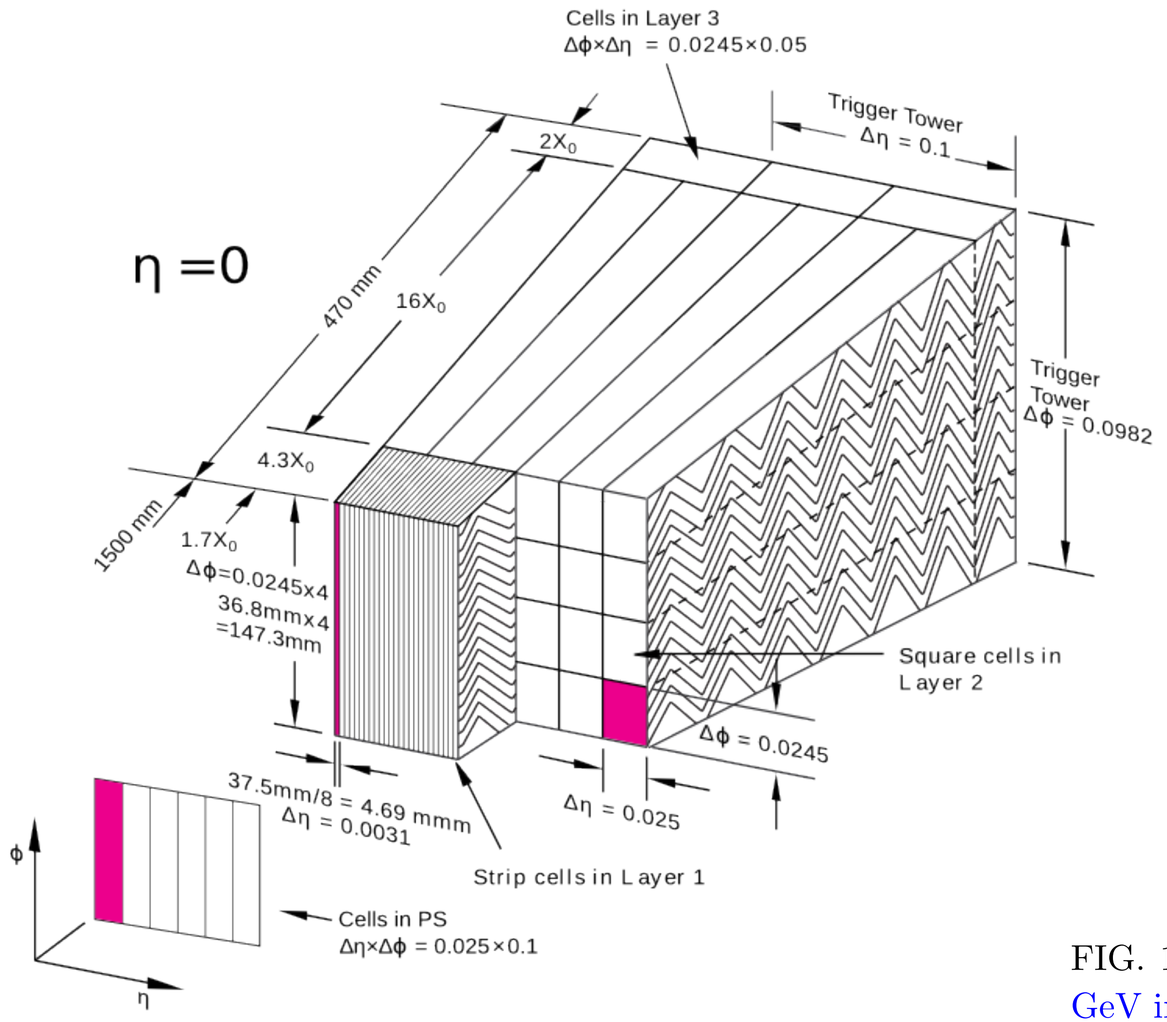

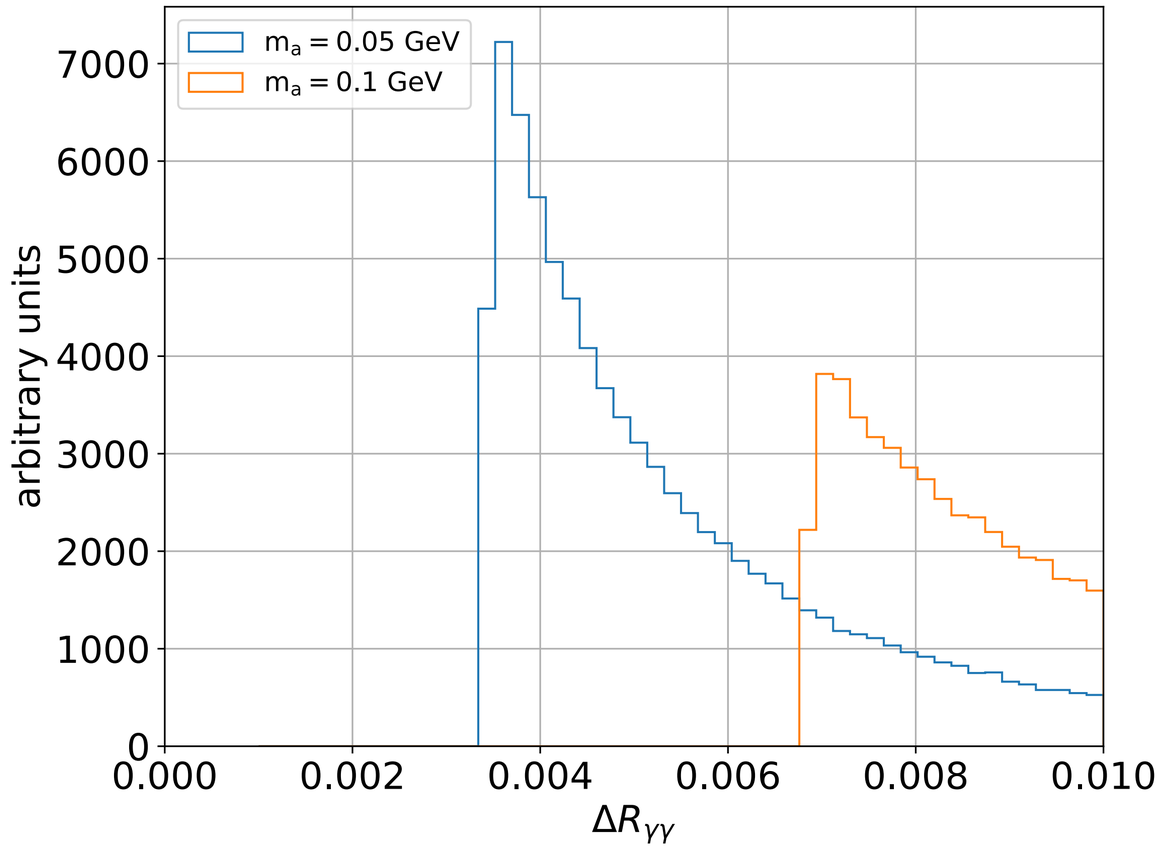

FIG. 1. Distributions of $\Delta R_{\gamma\gamma}$ between the photon pair produced for $m_a = 0.05$ GeV and 0
GeV in the decay $H \to Za \to (l^+l^-)\,(\gamma\gamma)$. It is clear the opening angle between the photon pair
very small.

- The possible mass range of ALP mass: $0.05 \leq m_a \leq 0.1\,\mathrm{GeV}$
- The upper mass range is due to the angular resolution of ECAL.
- The lower mass limit comes from constraints on $C_{\gamma\gamma}^{\mathrm{eff}}/\Lambda$
- Finally, $H \to Za \to (\ell^+\ell^-)(\gamma\gamma)_{\mathrm{collimated}}$ appears like $Z\gamma \to (\ell^+\ell^-)\gamma$
- The excess requires:

  $$B(H \to Za) = B(H \to Z\gamma)_{\mathrm{measured}} - B(H \to Z\gamma)_{\mathrm{sm}} = (1.9 \pm 1.1) \times 10^{-3}$$

- The effective coupling

  $C_{aZH}^{\mathrm{eff}} \approx 4.4 \times 10^{-2}\,\mathrm{TeV}^{-1}$ can explain the data.

Interactions

- ALP-gauge, fermions:

$$\mathcal{L}^{D=5} = \frac{1}{2}(\partial_\mu a)(\partial^\mu a) - \frac{1}{2}m_a^2 a^2 + \sum_f \frac{c_{ff}}{2\Lambda}\partial^\mu a\, \bar{f}\gamma_\mu\gamma_5 f$$
$$+ g_S^2\frac{C_{GG}}{\Lambda}aG^A_{\mu\nu}\tilde{G}^{\mu\nu,A} + g^2\frac{C_{WW}}{\Lambda}aW^i_{\mu\nu}\tilde{W}^{\mu\nu,i} + g'^2\frac{C_{BB}}{\Lambda}aB_{\mu\nu}\tilde{B}^{\mu\nu}$$

$$\mathcal{L} = e^2\frac{C_{\gamma\gamma}}{\Lambda}aF_{\mu\nu}\tilde{F}^{\mu\nu} + \frac{2e^2}{s_w c_w}\frac{C_{\gamma Z}}{\Lambda}aF_{\mu\nu}\tilde{Z}^{\mu\nu} + \frac{e^2}{s_w^2 c_w^2}\frac{C_{ZZ}}{\Lambda}aZ_{\mu\nu}\tilde{Z}^{\mu\nu}$$

- ALP-Higgs, ALP-Z-Higgs

$$\mathcal{L}^{D\geq 6} = \frac{C_{ah}}{\Lambda^2}(\partial_\mu a)(\partial^\mu a)\,\phi^\dagger\phi + \frac{C_{aZH}}{\Lambda^3}(\partial^\mu a)\,\left(\phi^\dagger i D_\mu\phi + \text{h.c.}\right)\,\phi^\dagger\phi\,,$$

$$D_\mu = \partial_\mu + i\frac{g}{\sqrt{2}}\left(W_\mu^+\tau^+ + W_\mu^-\tau^-\right) + ieQA_\mu + i\frac{g}{c_w}(T_3 - s_w^2 Q)Z_\mu\,,$$

- Why this obvious dim-5 term $\frac{C_5}{\Lambda}(\partial^\mu a)(\phi^\dagger D_\mu \phi + \mathrm{h.c.})$ does not appear?

  Consider:

$$\mathcal{L} = -\frac{c_{ff}}{\Lambda} m_f a\, \bar{f} i\gamma_5 f + \frac{C_5}{\Lambda}(\partial^\mu a)(\phi^\dagger i D_\mu \phi + h.c.)$$

  using the equation of motion:

$$\frac{C_5}{\Lambda}\partial^\mu(\phi^\dagger i D_\mu \phi + h.c.) = -\frac{c_{ff}}{\Lambda} m_f\, \bar{f} i\gamma_5 f$$

  - Using integration by parts and equation of motion, this dim-5 term is reduced to

$$(\partial^\mu a)\,(\phi^\dagger D_\mu \phi + \mathrm{h.c.}) \longrightarrow m_f\, a \bar{f} i\gamma_5\, f$$

  - This dim-5 operator does not appear. In another word, there exists an equivalent basis such that this operator do not contribute to $H \to Za$

  - So far, up to now $H \to Za$ is only given by the dim-7 operator:

$$\frac{C_{aZH}}{\Lambda^3}(\partial^\mu a)(\phi^\dagger D_\mu \phi + \mathrm{h.c.})(\phi^\dagger \phi)$$

- As familiar to the Higgs Low-Energy Theorem, in theories where a heavy new particles acquires mass via EWSB, the non-polynomial dim-5 operator can appear:

$$\frac{C_{aZH}^{(5)}}{\Lambda}(\partial^\mu a)(\phi^\dagger D_\mu \phi + \mathrm{h.c.})\ \ln(\phi^\dagger\phi/v^2)$$ [Bauer, Heiles, Neubert, Thamm 1808.10323]

- This is a dim-5 operator contributing to tree-level ALP-Z-H coupling
- Write the effective ALP-Z-H coupling as

$$C_{aZH}^{\mathrm{eff}} = C_{aZH}^{(5)} + \frac{C_{aZH} v^2}{2\Lambda^2}$$

- And the interaction can be written as, after the EWSB:

$$\mathscr{L}_{aZH} = \frac{C_{aZH}^{\mathrm{eff}}}{\Lambda}\frac{gv}{c_w}(\partial^\mu a) Z_\mu H$$

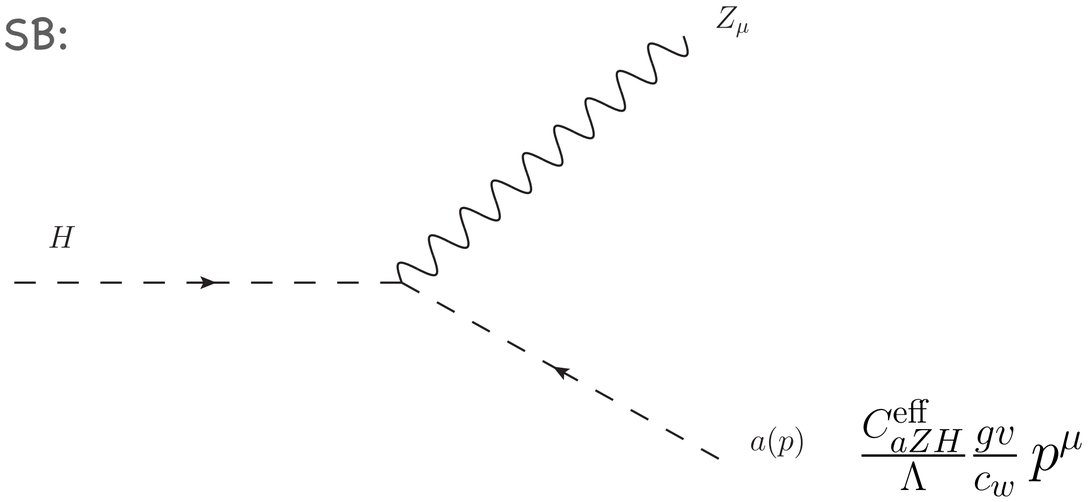

- We calculate the partial widths of $H \to Z\gamma$ and $H \to aa$

$$\Gamma(H \to Za) = \frac{m_H^3}{16\pi}\left(\frac{C_{aZH}^{\rm eff}}{\Lambda}\right)^2 \lambda^{3/2}(x_Z, x_a)$$

$$\Gamma(H \to aa) = \frac{m_H^3 v^2}{32\pi}\left(\frac{C_{aH}}{\Lambda^2}\right)^2 (1-2x_a)^2\sqrt{1-4x_a}$$

- The branching ratio for $H \to Za$:

$$B(H \to Za) = \frac{\Gamma(H \to Za)}{\Gamma(H \to Za) + \Gamma_{\rm sm}(m_H = 125\,{\rm GeV})} \,.$$

where $\Gamma_{\rm sm}(m_H = 125\,{\rm GeV}) = 4.088 \times 10^{-3}\,{\rm GeV}$

- Requiring the branching ratio to be $(1.9 \pm 1.1) \times 10^{-3}$, we found

$$C_{aZH}^{\rm eff}/\Lambda = (4.4^{+1.1}_{-1.6}) \times 10^{-2}\,{\rm TeV}^{-1}$$

- If the $C_{aZH}^{\rm eff} \sim O(1)$, then $\Lambda \approx 22.6\,{\rm TeV}$

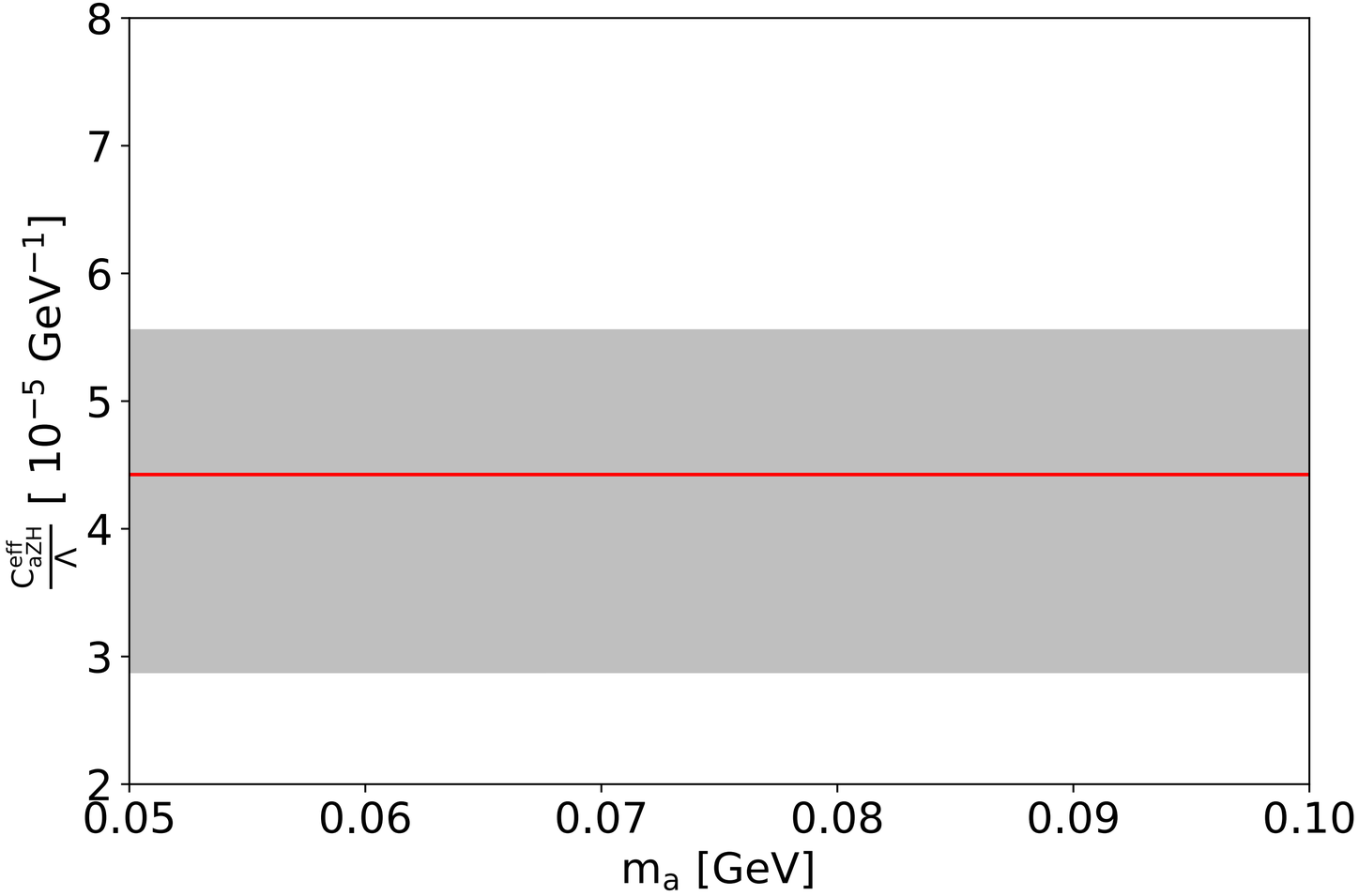

FIG. 3. The fitted values for $C^{\rm eff}_{aZH}/\Lambda$ versus m_a for $m_a = 0.05 - 0.1$ GeV. The red line and the band show the central value and 1σ uncertainty in $C^{\rm eff}_{aZH}/\Lambda = (4.4 \pm 1.1) \times 10^{-5}$ GeV^{-1} corresponding to $B(H \to Z\gamma) = (1.9 \times 1.1) \times 10^{-3}$.

Requirement on $C_{\gamma\gamma}^{\text{eff}}/\Lambda$ due to Decay Length of the ALP

- We require the ALP's decay length < 1.5 m, making sure that it decays before leaving the ECAL.
- Decay length $\gamma c\tau$ is

$$\gamma = E_a/m_a\,,\ \ \tau = 1/\Gamma_a\,,\quad \Gamma_a = 4\pi\alpha^2 m_a^3 \left(\frac{C_{\gamma\gamma}^{\text{eff}}}{\Lambda}\right)^2$$

- Taking $E_a \approx m_H/2$, the decay length requirement leads to

$$\frac{C_{\gamma\gamma}^{\text{eff}}}{\Lambda} \geq 0.35\,\text{TeV}^{-1} \left(\frac{0.1\,\text{GeV}}{m_a}\right)^2$$

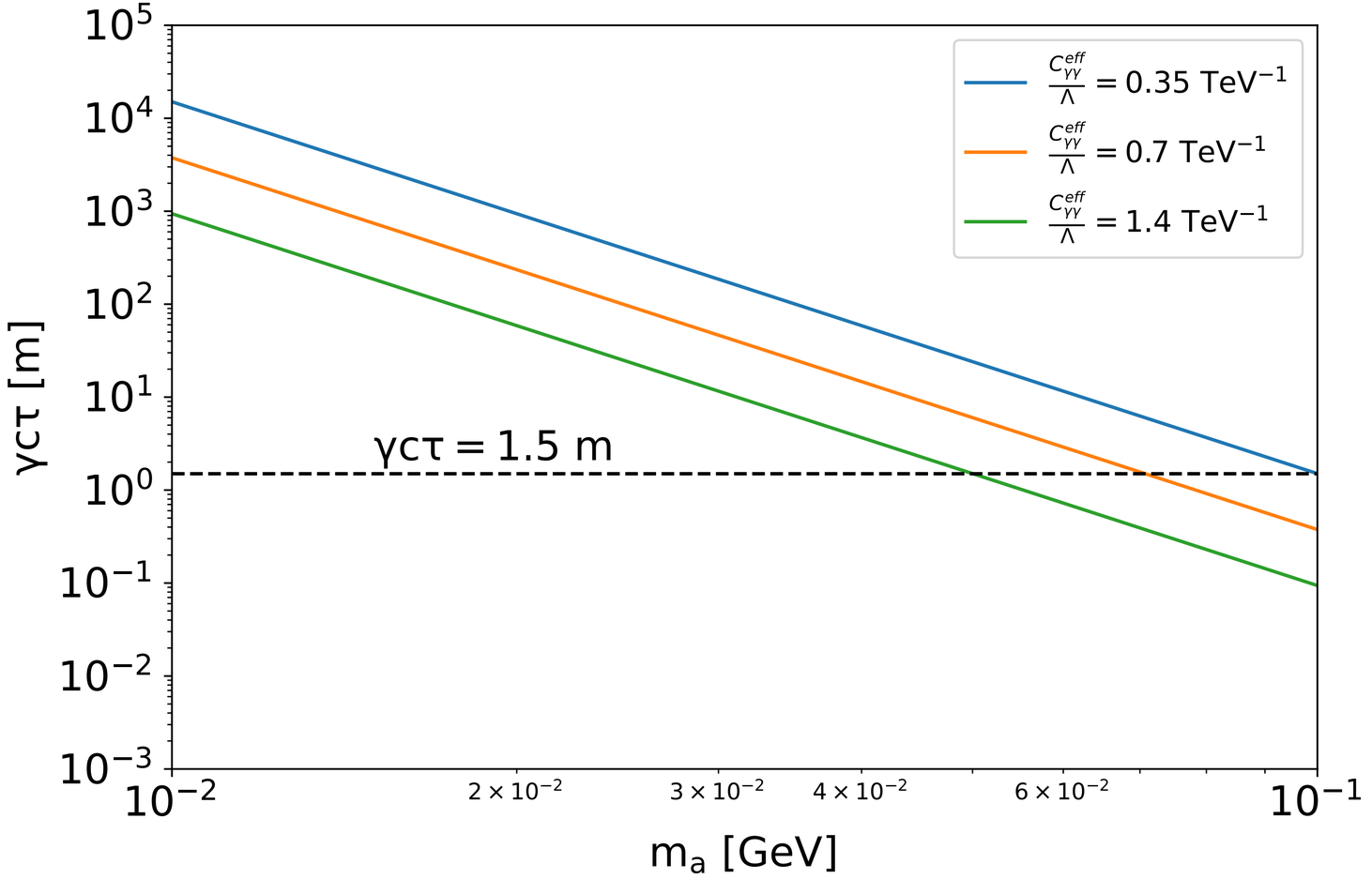

FIG. 4. Decay length $\gamma c\tau$ versus the mass m_a of the ALP. Values of $C_{\gamma\gamma}^{\rm eff}/\Lambda = 0.35,\ 0.7,\ 1.4\ \text{TeV}^{-1}$ are used. A dashed horizontal line of 1.5 m is also shown.

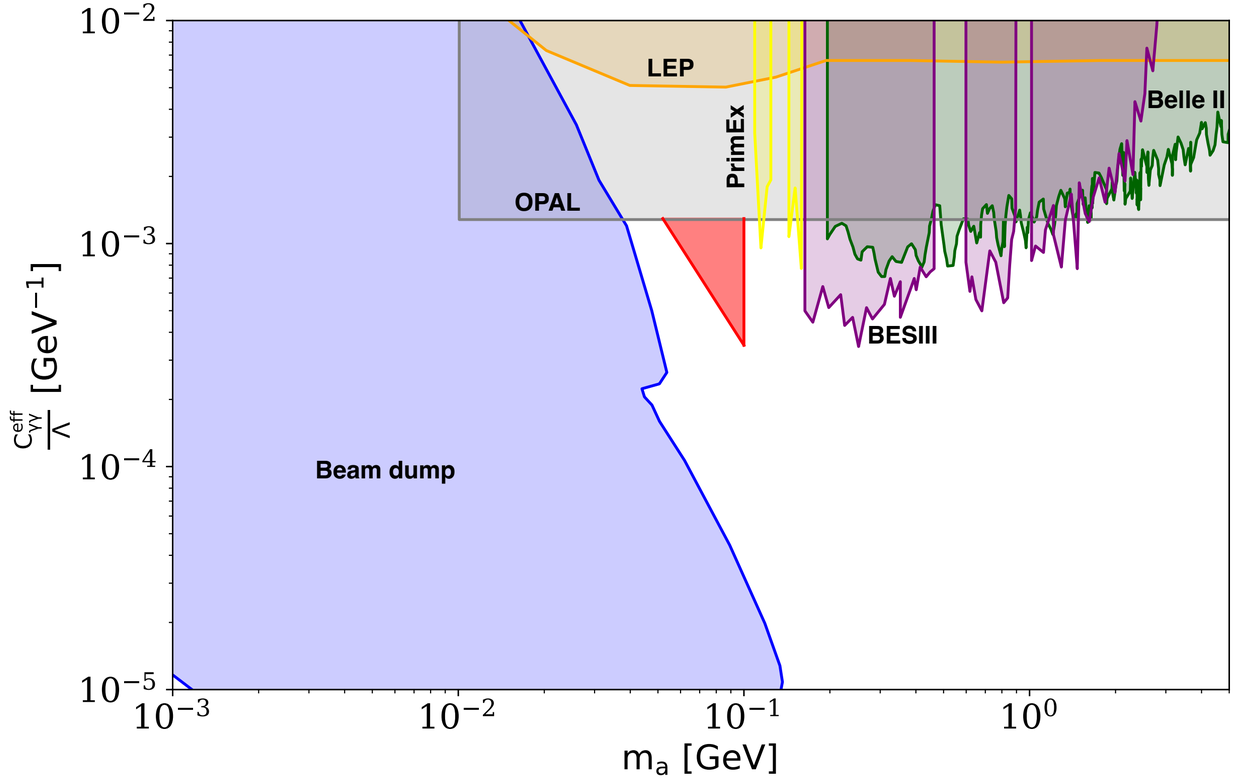

FIG. 5. Parameter space (shaded in red) in $C_{\gamma\gamma}^{\text{eff}}/\Lambda$ versus m_a that can allow the ALP to decay before reaching the ECAL (i.e. $\gamma c\tau \leq 1.5$ m) and consistent with all existing constraints in the mass range of $10^{-3} - 5$ GeV, including beam dump [40–44], OPAL [45], LEP [46], Belle II [47], BES III [48], and PrimEx [49] (data extracted from the GitHub page [50]). Note that the mass range of the fitted parameter space is $0.05\,\text{GeV} \leq m_a \leq 0.1\,\text{GeV}$.

For $m_a < 0.05\,\text{GeV}$, $C_{\gamma\gamma}^{\text{eff}}/\Lambda$ is restricted by current constraints.

For $m_a > 0.1\,\text{GeV}$, the ECAL may be able to resolve the photon pair.

Possible tests

1. $Z \to aH^* \to a(b\bar{b})$ via off-shell Higgs. The final state will be a collimated photon pair and a b quark pair. But the branching ratio is only 10^{-12}, which may give a few events at Tera-Z.

2. $pp \to Z^* \to aH$ via the same $C^{\text{eff}}_{aZH}/\Lambda$ coupling, but the cross section is 10^{-6} fb, which corresponds to far less than 1 event for entire HL run.

Summary

- $H \to Za,\ a \to \gamma\gamma$, where the ALP is very light 50 - 100 MeV, is a viable solution to the excess, without increasing $H \to \gamma\gamma$.
- It required a dim-5 vertex:

$$\frac{C^{(5)}_{aZH}}{\Lambda}(\partial^\mu a)(\phi^\dagger D_\mu \phi + \text{h . c.})\ \ln(\phi^\dagger\phi/v^2)$$

  which can arise in theories where a heavy new particles acquires mass via EWSB.
- It also requires the ALP to decay within the ECAL:

$$\frac{C^{\text{eff}}_{\gamma\gamma}}{\Lambda} \geq 0.35\,\text{TeV}^{-1}\left(\frac{0.1\,\text{GeV}}{m_a}\right)^2$$

Thank you (if time is limited)

Probing the ALP-gauge couplings at the LHC

K.C, Hsiao, Ouseph, Wang 2402.10550, JHEP 05 (2024) 324

ALP-Gauge Interactions

$$\mathcal{L} = \mathcal{L}_f + \mathcal{L}_g + \mathcal{L}_{BB} + \mathcal{L}_{WW}$$

$$\mathcal{L}_f = -\frac{ia}{f_a}\sum_f g_{af}\ m_f^{\rm diag}\bar{f}\gamma_5 f$$

$$\mathcal{L}_g = -C_g\frac{a}{f_a}G^A_{\mu\nu}\tilde{G}^{\mu\nu,A}$$

$$\mathcal{L}_{BB} = -C_{BB}\frac{a}{f_a}B_{\mu\nu}\tilde{B}^{\mu\nu}$$

$$\mathcal{L}_{WW} = -C_{WW}\frac{a}{f_a}W^i_{\mu\nu}\tilde{W}^{\mu\nu,i},$$

$$\begin{pmatrix} W^3_\mu \\ B_\mu \end{pmatrix} = \begin{pmatrix} c_w & s_w \\ -s_w & c_w \end{pmatrix}\begin{pmatrix} Z_\mu \\ A_\mu \end{pmatrix},$$

$$\mathcal{L} = -\frac{ia}{f_a}\sum_f g_{af}m_f^{\rm diag}\bar{f}\gamma_5 f - C_g\frac{a}{f_a}G^A_{\mu\nu}\tilde{G}^{\mu\nu A} - \frac{a}{f_a}\big[(C_{BB}c_w^2 + C_{WW}s_w^2)F_{\mu\nu}\tilde{F}_{\mu\nu} +$$
$$(C_{BB}s_w^2 + C_{WW}c_w^2)Z_{\mu\nu}\tilde{Z}_{\mu\nu} + 2(C_{WW} - C_{BB})c_w s_w F_{\mu\nu}\tilde{Z}_{\mu\nu} + C_{WW}W^+_{\mu\nu}\tilde{W}^{-\mu\nu}\big]\,.$$

$$g_{a\gamma\gamma} = \frac{4}{f_a}(C_{BB}c_w^2 + C_{WW}s_w^2),$$

$$g_{aWW} = \frac{4}{f_a}C_{WW},$$

$$g_{aZZ} = \frac{4}{f_a}(C_{BB}s_w^2 + C_{WW}c_w^2),$$

$$g_{aZ\gamma} = \frac{8}{f_a}s_w c_w(C_{WW} - C_{BB})\,.$$

- Associated production of the ALP with a Z / W boson:

$$pp \to \gamma^*, Z^* \to Za \to (\ell^+\ell^-)(\gamma\gamma)$$

$$pp \to W^* \to Wa \to (\ell\nu)(\gamma\gamma)$$

- The first process can probe $g_{a\gamma\gamma}$, $g_{aZ\gamma}$.
- The second process probes g_{aWW}.
- In this work, we probe $m_a = 1 - 100\,\mathrm{GeV}$, divided into two regions:

$$m_a \leq 25\,\mathrm{GeV} \quad \text{and} \quad 25 < m_a \leq 100\,\mathrm{GeV}$$

- Below 25 GeV the photon pair is close to each other. It appears as photon-jet.
- The backgrounds processes are also different for these 2 regions:

$$m_a \leq 25\,\mathrm{GeV} \quad \text{and} \quad 25 < m_a \leq 100\,\mathrm{GeV}$$

$$pp \to \gamma^*, Z^* \to Za \to (\ell^+\ell^-)(\gamma\gamma)$$

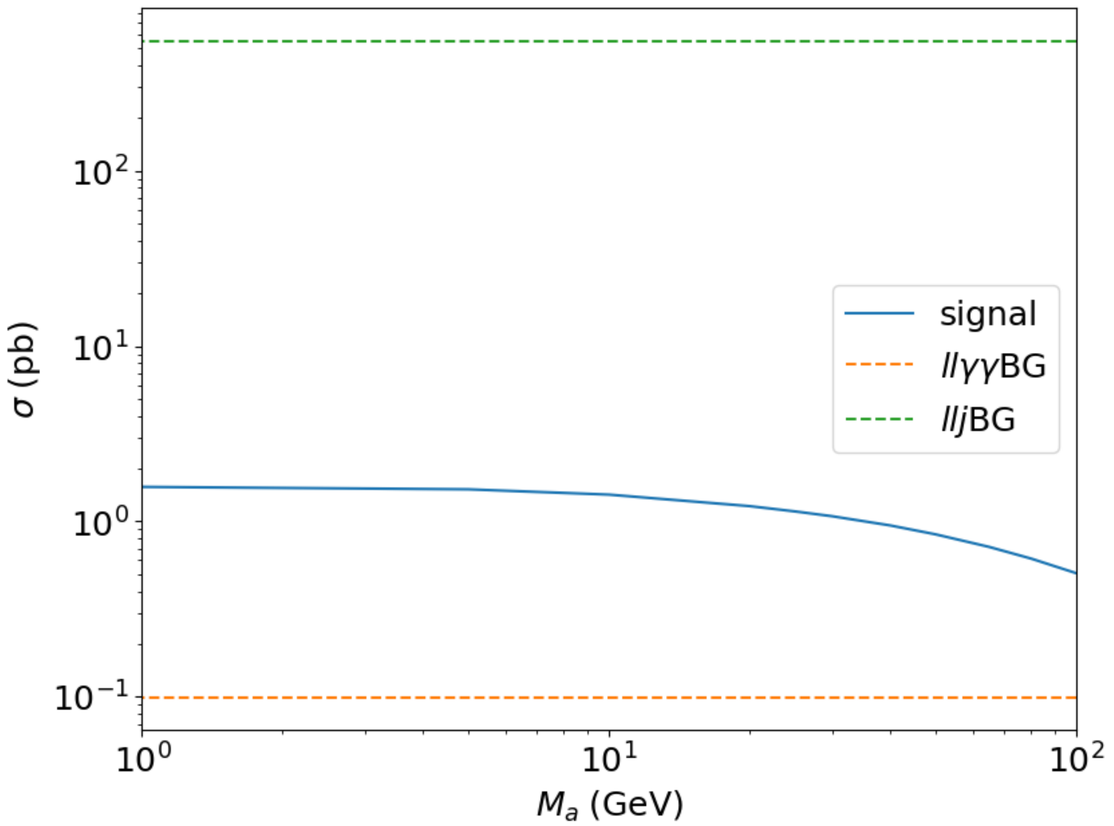

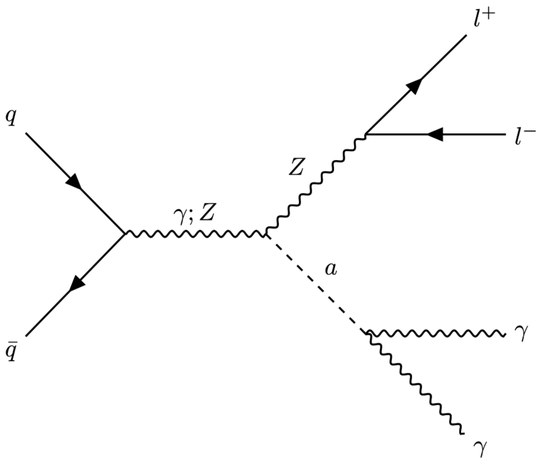

$$f_a = 1\,\text{TeV},\ C_{WW} = 2,\ C_{BB} = 1$$

$$p_{T_\gamma} > 10\,\text{GeV}, \quad |\eta_\gamma| < 2.5\,,$$
$$p_{T_l} > 10\,\text{GeV}, \quad |\eta_l| < 2.5\,,$$
$$p_{T_j} > 20\,\text{GeV}, \quad |\eta_j| < 2.5\,, R_{\text{cone}} = 0.4\,,$$
$$\Delta R_{ab} = 0.4 \quad \text{where} \quad a, b = \gamma, l, j\,.$$

Figure 2. Production cross section for $pp \to Za\ (Z \to l^+\ l^-)(a \to \gamma\gamma)$ with $l = e, \mu$ versus M_a, including the branching ratios at $\sqrt{s} = 14\,\text{TeV}$. Here we also show the backgrounds $ll\gamma\gamma$BG and lljBG.

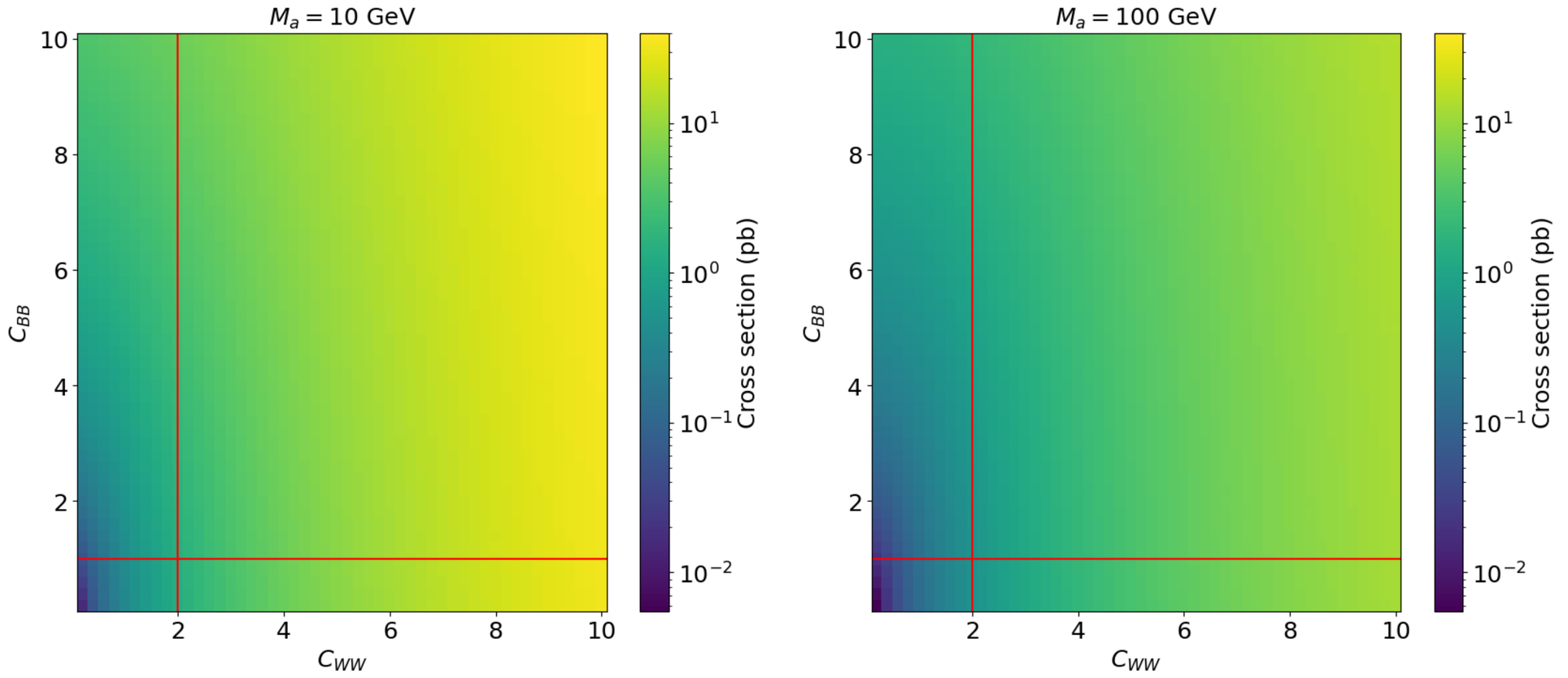

Figure 3. Cross sections for $pp \to Za\ (Z \to l^+\ l^-)(a \to \gamma\gamma)$ by varying the parameters C_{WW} and C_{BB} with $\sqrt{s} = 14$ TeV, $f_a = 1$ TeV and $M_a = 10$ or 100 GeV. The cross point of the two red lines represents the benchmark in our study, $C_{WW} = 2$ and $C_{BB} = 1$.

Signal-Background Analysis

- $m_a > 25\,\text{GeV}$
  1. $pp \to \ell^+\ell^-\gamma\gamma$ $(ll\gamma\gamma BG)$
  2. $pp \to \ell^+\ell^-\gamma j$, with $f_{j\to\gamma} \simeq 5\times10^{-4}$ $(ll\gamma jBG)$

- two photon selection
- two lepton selection
- 80 GeV $< M_{ll} <$ 100 GeV
- $p_{T_{\gamma\gamma}} > 80$ GeV
- $0.9M_a < M_{\gamma\gamma} < 1.1M_a$

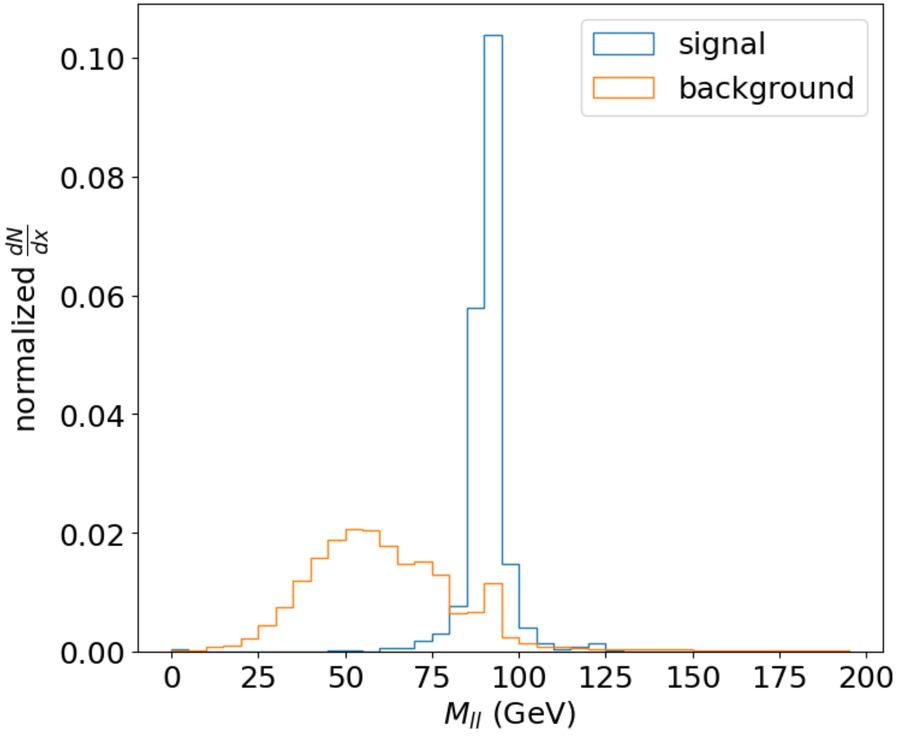

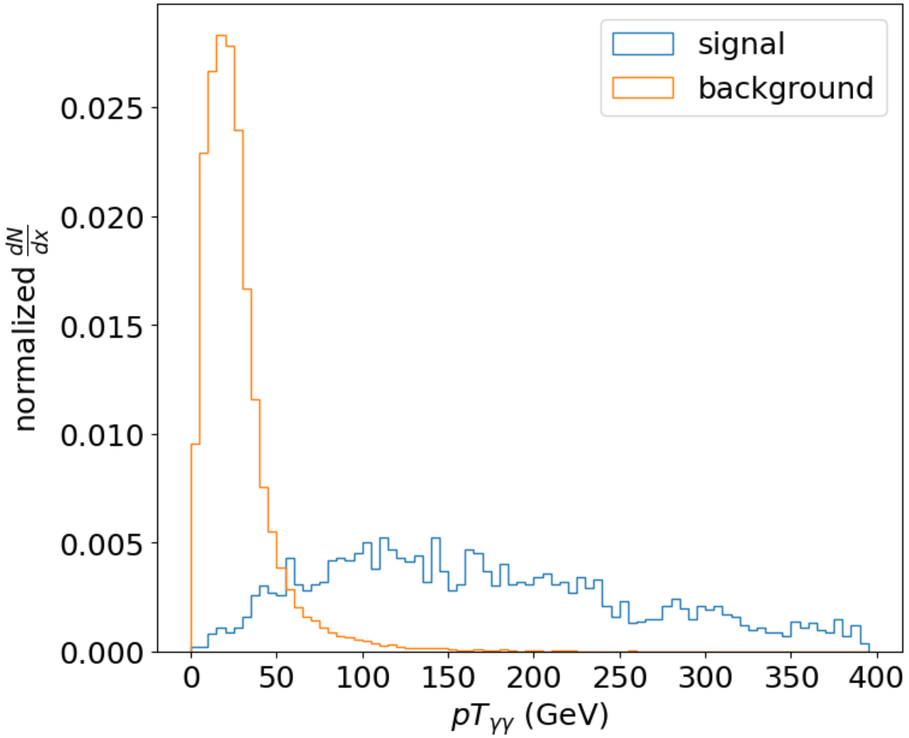

$m_a = 100$ GeV

Selection	**Signal**	$ll\gamma\gamma$**BG**	$ll\gamma j$**BG**
Before cuts	151948	29728	1048
$N(\gamma) = 2$	69243	12387	61.30
$N(l) = 2$	32152	5488	2.83
80 GeV $< \mathrm{M_{ll}} <$ 100 GeV	29584	739	0.60
$pT_{\gamma\gamma} >$ GeV	24965	90	0.05
90 GeV $< \mathrm{M}_{\gamma\gamma} <$ 110 GeV	24707	13	0.02

Table 1. Cut flow for the signal ($pp \to Za$) with $Z \to l^+l^-$ and $a \to \gamma\gamma$ and the background process ($pp \to l^+l^-\gamma\ \gamma$) and ($pp \to l^+l^-\gamma j$) with $M_a = 100$ GeV, with $f_a = 1$ TeV, $C_{WW} = 2$, $C_{BB} = 1$, and $C_g = g_{af} = 0$. "Before cuts" in the first row denotes the total number of events with only the parton-level cuts with the integrated luminosity of $300\,\mathrm{fb}^{-1}$ calculated by eq. (4.1). In $ll\gamma j$BG, we have applied the jet-fake rate $f_{j\to\gamma} = 5 \times 10^{-4}$.

- $m_a \leq 25\,\mathrm{GeV}$
  1. $pp \to \ell^+\ell^-\gamma\gamma$ $(ll\gamma\gamma BG)$
  2. $pp \to \ell^+\ell^- j, \quad (lljBG)$

- At least one jet
- $min(\frac{E_{had}}{E_{\mathrm{EM}}}) < 0.02$
- two lepton selection
- $80\ \mathrm{GeV} < M_{ll} < 100\ \mathrm{GeV}$
- $\frac{\tau_2}{\tau_1} < 0.05$
- M_{jet} mass window

M_a (GeV)	$M_{\mathbf{jet}}$ **selection** (GeV)
25	$22.5 < M_{\mathrm{jet}} < 30$
20	$18 < M_{\mathrm{jet}} < 24$
10	$9 < M_{\mathrm{jet}} < 12$
5	$4.5 < M_{\mathrm{jet}} < 6$
1	$0.5 < M_{\mathrm{jet}} < 2$

Table 2. M_{jet} mass window for the low ALP mass region.

- The photon pair from ALP decay forms a photon-jet, the majority of energy is deposited in ECAL.
- There are multi-jet background. A quantity $E_{\mathrm{had}}/E_{\mathrm{em}}$ is defined for each jet. We require

$$\min(E_{\mathrm{had}}/E_{\mathrm{em}}) < 0.02$$

- Nsubjettiness τ_N defined by

$$\tau_N = \frac{1}{d_0}\sum_k p_{T,k}\min\left\{\Delta R_{1,k}, \Delta R_{2,k}, \ldots, \Delta R_{N.k}\right\}, \quad \Delta R_{j,k} = \sqrt{(\Delta\eta)^2 + (\Delta\phi)^2}, \quad d_0 = \sum_k p_{T,k} R_0$$

- $\frac{\tau_N}{\tau_{N-1}}$ is a useful parameter to determine if a jet consists of N substructure.

- The ideal ALP jet consists of 2 photons w/o any initial radiation, which gives $\tau_2 = 0, \tau_1 \neq 0$. So we require $\tau_2/\tau_1 < 0.05$.
- The asymmetric jet-mass window is motivated by the acceptance of initial radiation.

$m_a = 10$ GeV

Selection	**Signal**	$ll\gamma\gamma$ **BG**	llj **BG**
Before cuts	426413	29728	164921970
$N(jet) \geq 1$	356610	17327	139649327
$min(\frac{E_{had}}{E_{\mathrm{EM}}}) < 0.02$	267532	8150	26141121
$N(l) = 2$	88523	1169	649627
80 GeV $< \mathrm{M_{ll}} <$ 100 GeV	81957	181	460297
$\frac{\tau_2}{\tau_1} < 0.05$	62811	46	36613
9 GeV $< \mathrm{M_{jet}} <$ 12 GeV	48995	0	0

Explanation of N-subjettiness

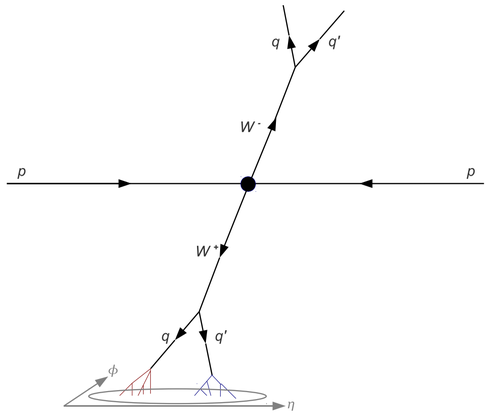

(a)

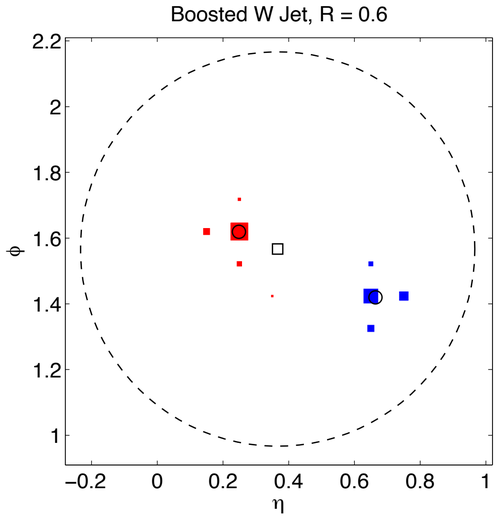

(b)

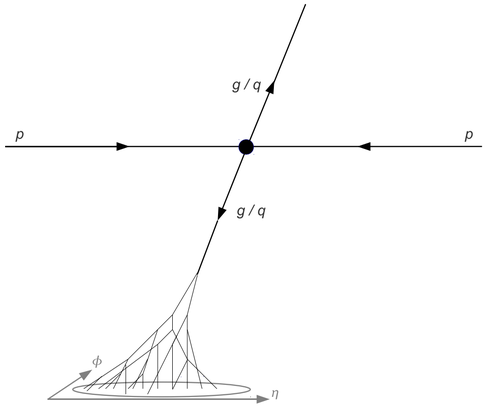

(c)

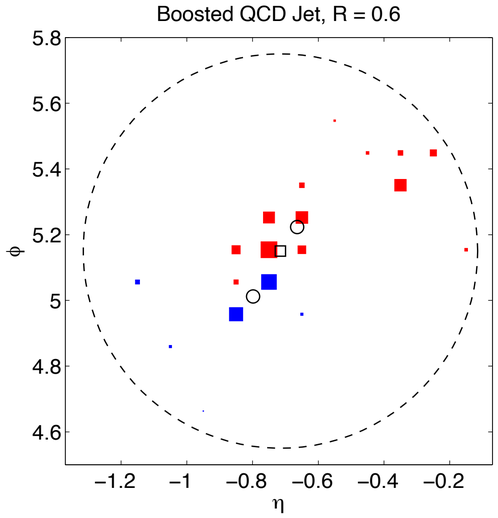

(d)

Jets with $\tau_N \approx 0$ have all their radiation aligned with the candidate subjet directions and therefore have N (or fewer) subjets. Jets with $\tau_N \gg 0$ have a large fraction of their energy distributed away from the candidate subjet directions and therefore have at least N + 1 subjets.

$\tau_2/\tau_1 \ll 1$ is a measure of 2-jet substructure.

$$pp \to W^* \to Wa \to (\ell\nu)(\gamma\gamma)$$

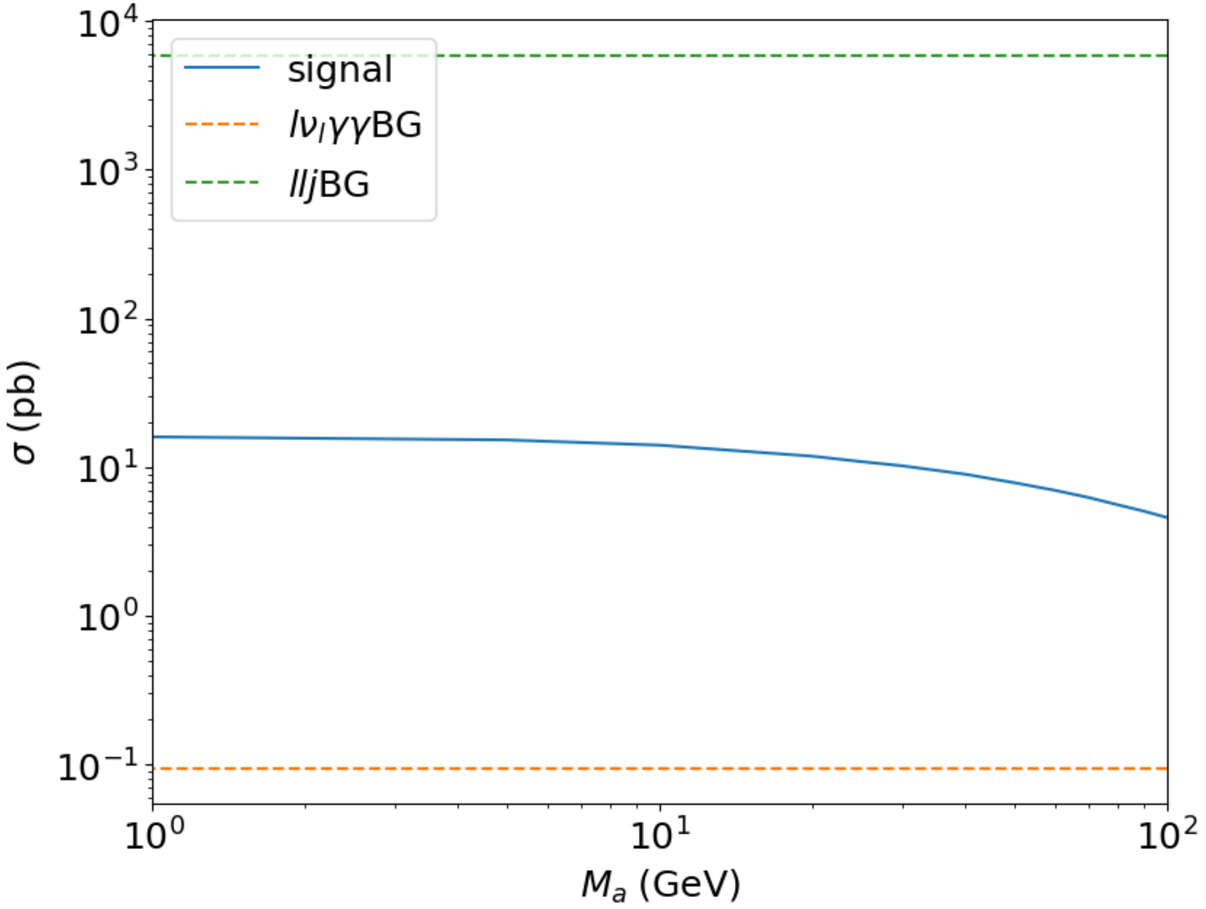

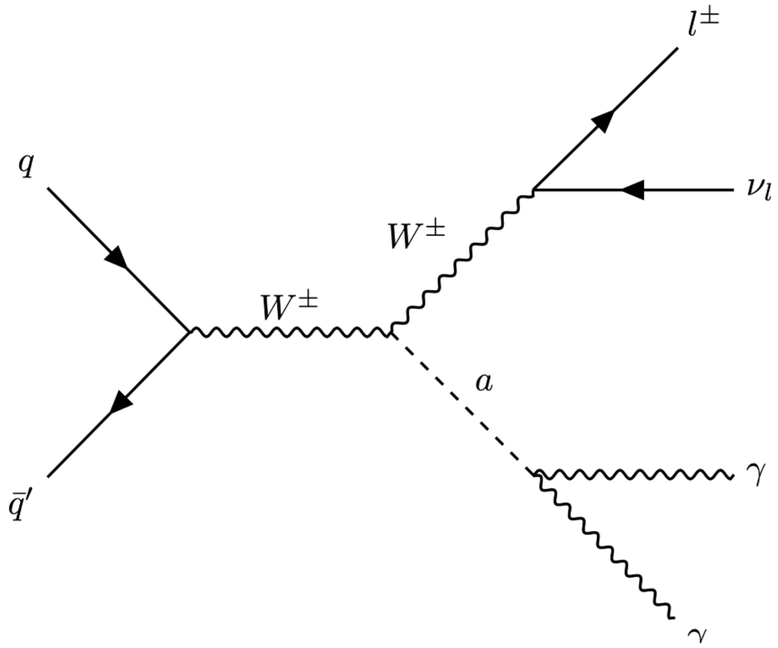

$f_a = 1\,\text{TeV}$, $C_{WW} = 2$, $C_{BB} = 1$

Figure 5. Production cross sections for $pp \to W^\pm a\,(W^\pm \to l^\pm \nu_l)\,,(a \to \gamma\gamma)$ with $l = e, \mu$ versus M_a at $\sqrt{s} = 14\,\text{TeV}$, including branching ratios. Here we also show $l\nu_l\gamma\gamma$BG and $l\nu_l j$BG.

Signal-Background Analysis

- $m_a > 25\,\mathrm{GeV}$
  1. $pp \to \ell\nu\gamma\gamma$ $(l\nu\gamma\gamma BG)$
  2. $pp \to \ell\nu\gamma j$, with $f_{j\to\gamma} \simeq 5\times10^{-4}$ $(l\nu\gamma jBG)$

- two photon selection
- one lepton selection
- $p_{T_{\gamma\gamma}} > 50$ GeV
- $M_T > 58$ GeV
- $0.9M_a < M_{\gamma\gamma} < 1.1M_a$

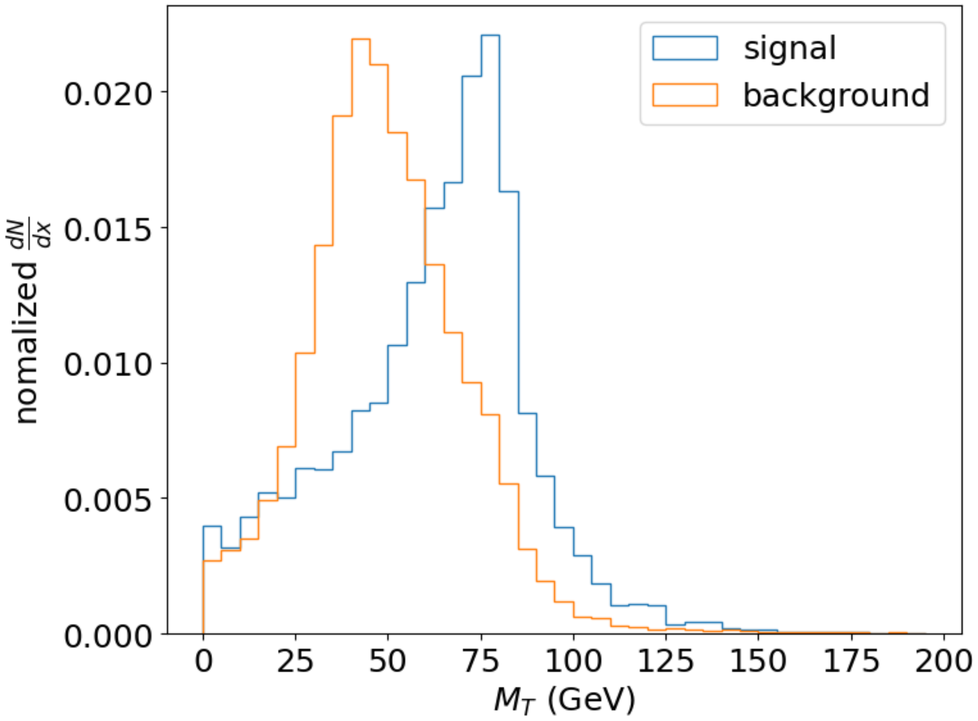

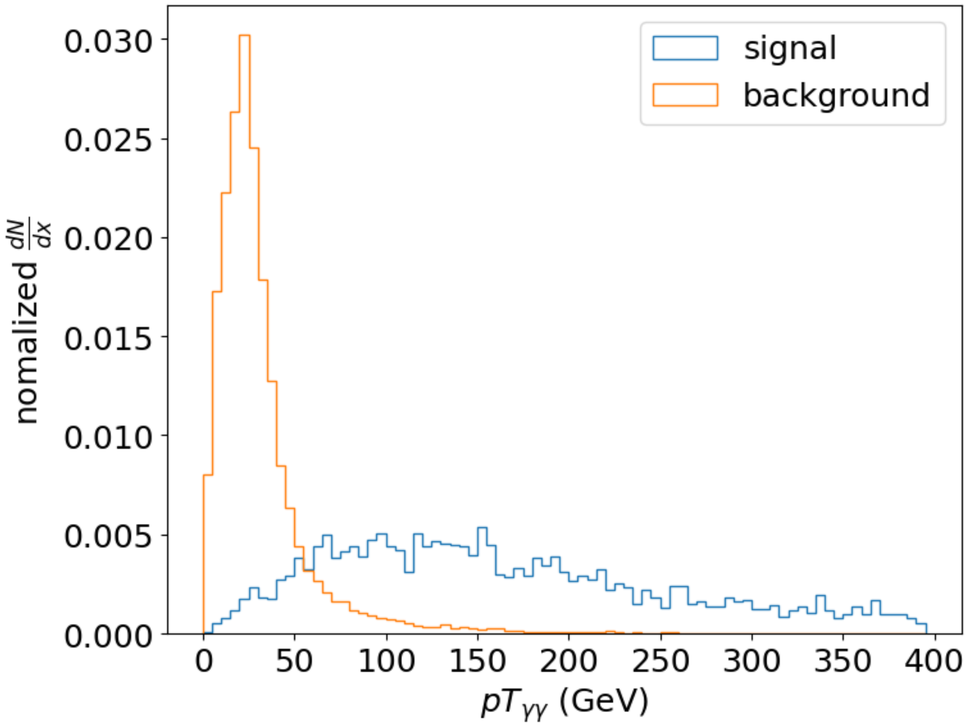

$m_a = 100$ GeV

Selection	**Signal**	$l\nu_l\gamma\gamma$ **BG**	$l\nu_l\gamma j$ **BG**
Before cuts	1375200	28311	5268
$N(\gamma) = 2$	617190	11435	152.2
$N(l) = 1$	402521	6954	12.3
$pT_{\gamma\gamma} > 50$ GeV	372542	906	3.5
$M_T > 58$ GeV	232821	441	1.8
$90 < M_{\gamma\gamma} < 110$	230208	48	0.16

Table 4. Cut flow for the signal $pp \to W^{\pm}a$ and the background $(pp \to l\nu_l\gamma\gamma)$ and $(pp \to l\nu_l\gamma j)$ with $M_a = 100$ GeV, with couplings $f_a = 1$ TeV, $C_{WW} = 2$, $C_{BB} = 1$, and $C_g = g_{af} = 0$. "Before cuts" in the first row denotes the total number of events with only the parton-level cuts computed using eq. (4.1), with the signal and background cross sections given in figure 5 and the luminosity set at $\mathcal{L} = 300$ fb^{-1}. In $l\nu_l\gamma j$BG, we have applied the jet-fake rate $f_{j\to\gamma} = 5 \times 10^{-4}$.

- $m_a \leq 25\,\text{GeV}$
  1. $pp \to \ell\nu\gamma\gamma$ ($l\nu\gamma\gamma BG$)
  2. $pp \to \ell\nu j$ ($l\nu jBG$)

- At least one jet
- $min(\frac{E_{had}}{E_{\text{EM}}}) < 0.02$
- one lepton selection
- $M_T > 58$ GeV
- $\frac{\tau_2}{\tau_1} < 0.05$
- M_{jet} mass window

Selection	**Signal**	$l\nu_l\gamma\gamma$ **BG**	$l\nu_l j$ **BG**
Before cuts	4218000	28311	1766100000
$N(jet) \geq 1$	3289618	13415	1468625180
$min(\frac{E_{had}}{E_{\rm EM}}) < 0.02$	2782193	6824	250477133
$N(l) = 1$	1412608	2235	26117087
$M_T > 58$ GeV	888733	765	16493608
$\frac{\tau_2}{\tau_1} < 0.05$	595160	200	665820
9 GeV $<$ $\rm M_{jet}$ $<$ 12 GeV	461449	2	1766

Table 5. Cut flow for the signal $pp \to W^{\pm}\, a$ and backgrounds $pp \to l\nu_l\gamma\gamma$ and $pp \to l\nu_l j$ with $M_a = 10$ GeV, featuring couplings $f_a = 1$ TeV, $C_{WW} = 2$, $C_{BB} = 1$, and $C_g = g_{af} = 0$. "Before cuts" in the first row denotes the total number of events with only the parton-level cuts computed using eq. (4.1), with the signal and background cross sections given in figure 5 and the luminosity set at $\mathcal{L} = 300$ fb^{-1}.

Signal and Background events of $pp \to Za$ for $m_a = 1 - 100$ GeV

M_a (GeV)	**Signal**		$ll\gamma\gamma$**BG**+$ll\gamma j$**BG**		llj**BG**	
	before	after	before	after	before	after
100	151947	24707		12.80		
80	184160	25211		12.78		
65	214813	23522		7.13		
50	253073	23207	30775	4.16	-	
40	284456	19286		3.87		
30	321176	12205		2.97		
25	342005	25206		0		0
20	366568	34311		0		0
10	426413	48995	29728	0	164950770	0
5	457138	48914		0.59		165
1	472141	46175		29.43		18474

Table 6. Total number of signal events for $pp \to Za$, followed by $Z \to l^+l^-, a \to \gamma\gamma$ and background events of $ll\gamma\gamma$BG and lljBG for the mass range $M_a = 1 - 100$ GeV. The number of events are calculated by eq. (4.1), where the cross sections of signal and backgrounds are shown in figure 2 and the integrated luminosity is set at $\mathcal{L} = 300$ fb^{-1}.

- the signal events with $f_a = 1\,\text{TeV}$, $C_{WW} = 2$, $C_{BB} = 1$

Signal and Background events of $pp \to W^{\pm}a$ for $m_a = 1 - 100$ GeV

M_a (GeV)	**Signal**		$l\nu_l\gamma\gamma$**BG** $+l\nu_l\gamma j$**BG**		$l\nu_l j$**BG**	
	before	after	before	after	before	after
100	1375200	230208		48.01		
80	1674900	244870		52.87		
65	1992000	261151		57.09		
50	2357400	245170	33579	36.57		
40	2690700	220906		26.43		
30	3066000	193771		21.05		
25	3267000	224443		0		0
20	3555000	290799		0.57		0
10	4218000	461449	28311	1.98	1766100000	1766
5	4575000	522007		6.79		17661
1	4797000	469147		110		326729

Table 7. Total number of signal events for $pp \to W^{\pm}a$, followed by $W^{\pm} \to l^{\pm}\nu_l, a \to \gamma\gamma$ and background events of $l\nu_l\gamma\gamma$BG and $l\nu_l j$BG for the mass range $M_a = 1 - 100$ GeV. The number of events are calculated by eq. (4.1), where the cross sections of signal and backgrounds are shown in figure 5 and the integrated luminosity is set at $\mathcal{L} = 300$ fb^{-1}.

- the signal events with $f_a = 1\,\text{TeV}$, $C_{WW} = 2$, $C_{BB} = 1$

Sensitivity Estimation

- So far we illustrated the signal events with $f_a = 1\,\mathrm{TeV}$, $C_{WW} = 2$, $C_{BB} = 1$.
- We use simple scaling:

$$s \propto 1/f_a^2 \propto g_{aZZ}^2, g_{aZ\gamma}^2, g_{aWW}^2$$

- The significance of the signal is

$$Z = \sqrt{2\left[(s+b)\ln\left(\frac{(s+b)(b+\sigma_b^2)}{b^2+(s+b)\sigma_b^2}\right) - \frac{b^2}{\sigma_b^2}\ln\left(1+\frac{\sigma_b^2 s}{b(b+\sigma_b^2)}\right)\right]}$$

where s, b are signal and background events, $\sigma_b = 0\,\%$ and $10\,\%$ of b

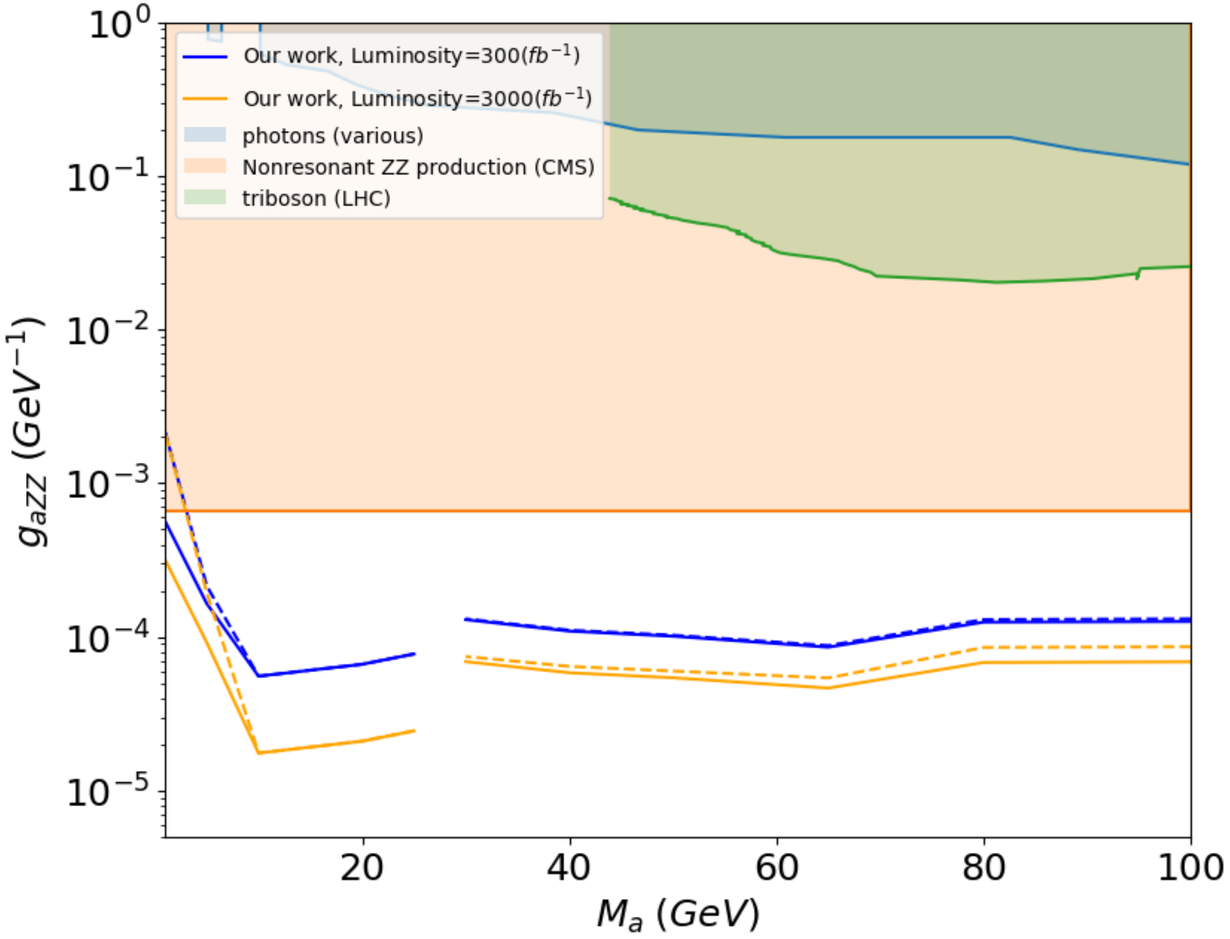

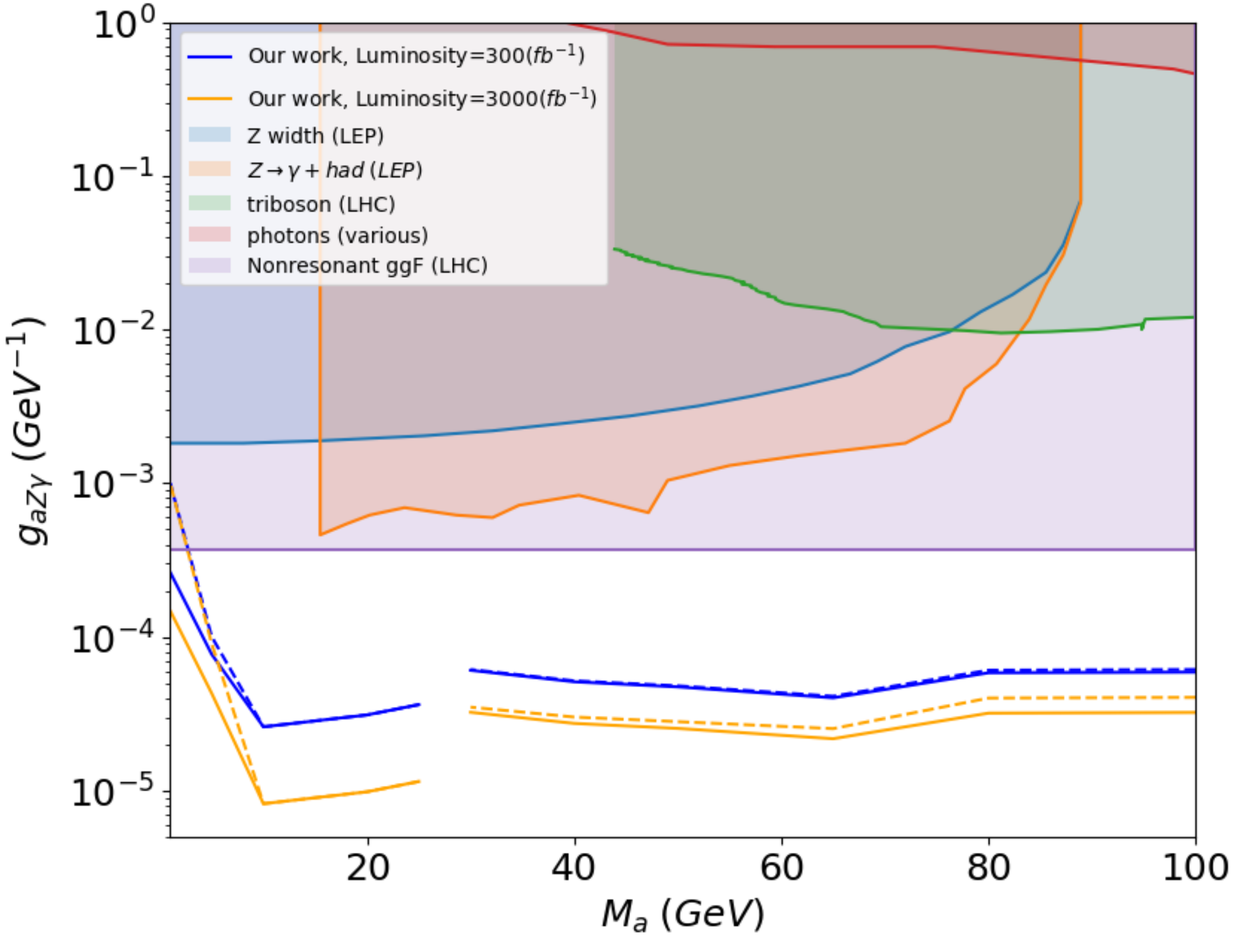

$$s, b = \sigma_{s,b} \times \frac{N_{\text{selected}}}{N_{\text{sim}}} \times \mathcal{L}.$$

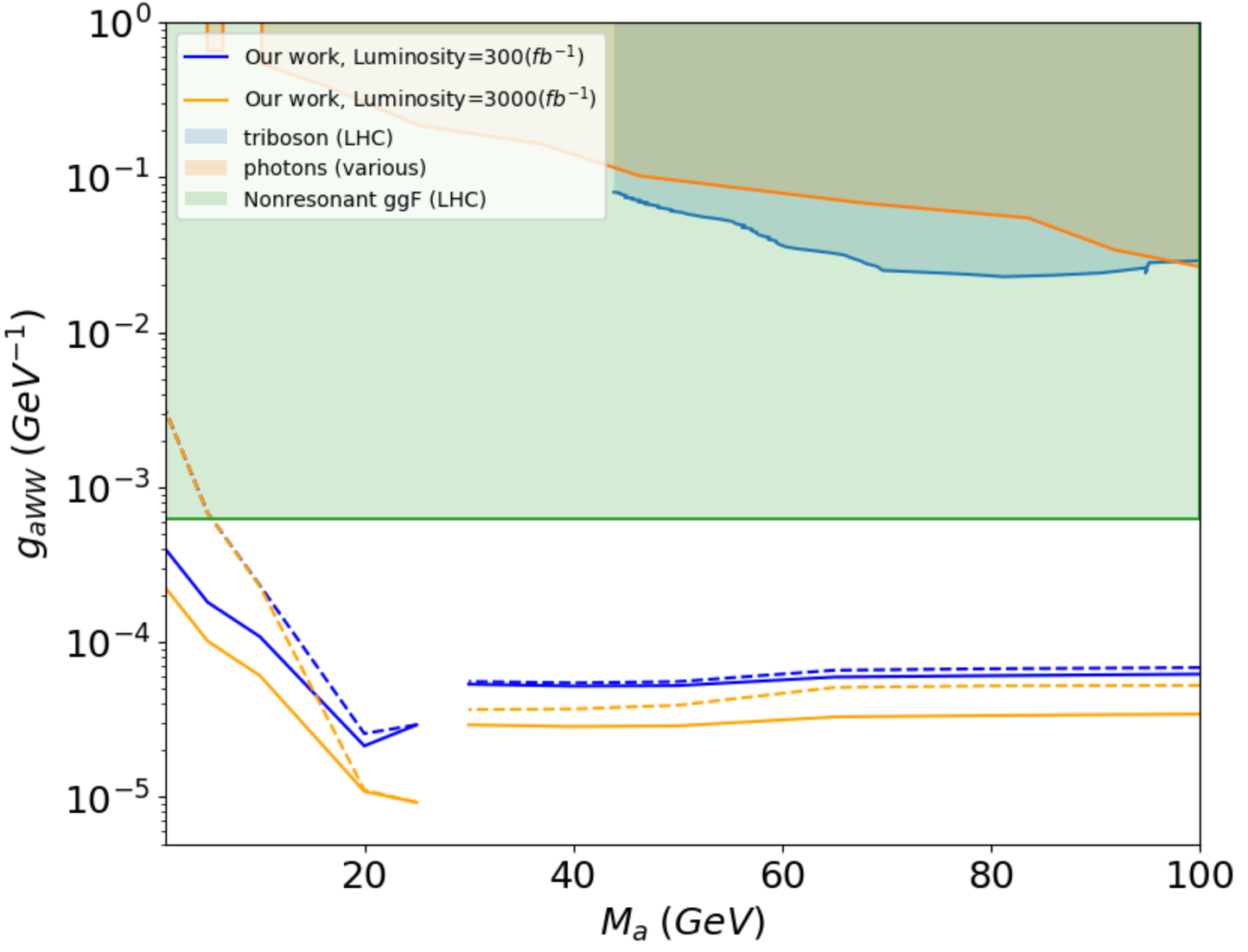
Our work, Luminosity=300(fb^{-1})
Our work, Luminosity=3000(fb^{-1})
triboson (LHC)
photons (various)
Nonresonant ggF (LHC)
10^0
10^{-1}
10^{-2}
10^{-3}
10^{-4}
10^{-5}
g_{aWW} (GeV^{-1})
20
40
60
80
100
M_a (GeV)

Simultaneous Sensitivity in C_{WW}, C_{BB}

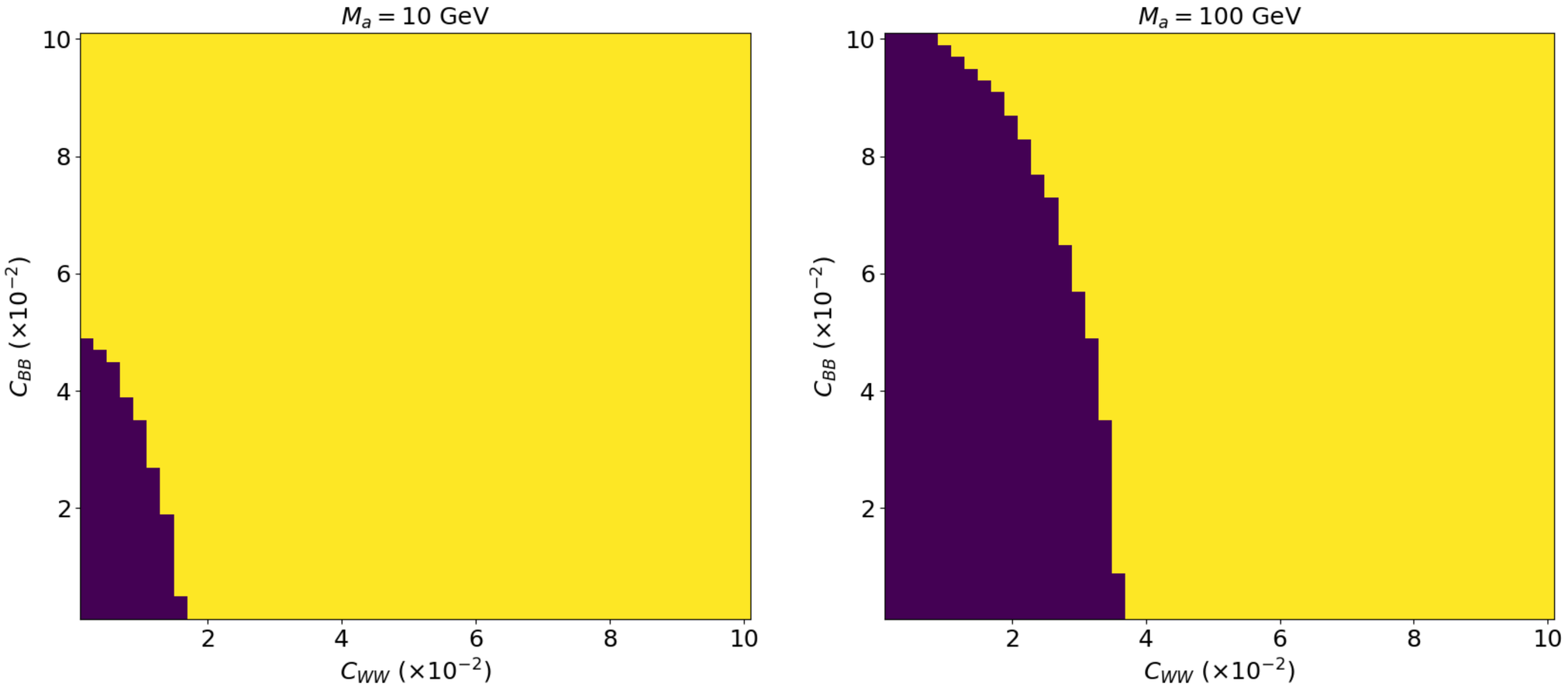

Figure 8. Sensitivity plot in the plane of (C_{WW}, C_{BB}) for $M_a = 10\,\text{GeV}$ (left panel) and for $M_a = 100\,\text{GeV}$ (right panel). We fix $f_a = 1\,\text{TeV}$. The bright region on the left panel is for the number of signal events > 3 in case with zero background, while that on the right panel is for significance $Z > 2$. Note that the signal cross section scales as $1/f_a^2$.

Explanations for Existing Constraints

- Various collider constraints on ALP-photon coupling $g_{a\gamma\gamma}$ can be converted into $g_{aZZ}, g_{aZ\gamma}, g_{aWW}$ using the SU(2) relations. They are labeled as "photon (various)".
- FCNC interactions of the ALP are constrained by invisible and visible decay of Kaon and B mesons. Invisible ALP contributes to $K \to \pi\nu\bar{\nu}$, visible ALP contributes to DV in $B \to K^*\mu^+\mu^-$.
- "Triboson (LHC)" :: cross sections of $pp \to WZ\gamma, Z\gamma\gamma, WZZ, Z\gamma\gamma, ZZZ, \ldots$. It constrains all g's.
- Constraints on $g_{aZ\gamma}$ by non-SM Z decay $\Gamma(Z \to BSM) \leq 2\,\mathrm{MeV}$, by $Z \to \gamma + \mathrm{hadron}$, by $Z \to \gamma\gamma$.
- Non-resonant ggF production of ALP via $gg \to a^* \to ZZ, Z\gamma, W^+W^-$

Summary

- Substantial improvements in sensitivity reach of g_{aZZ}, $g_{aZ\gamma}$, g_{aWW}.
- We divide the mass range into 2 parts, less or more than 25 GeV up to 100 GeV.
- For less than 25 GeV, we treat the collimated photons as a photon-jet.

Backup slides

Interference effects between ALP-gauge, ALP-top couplings

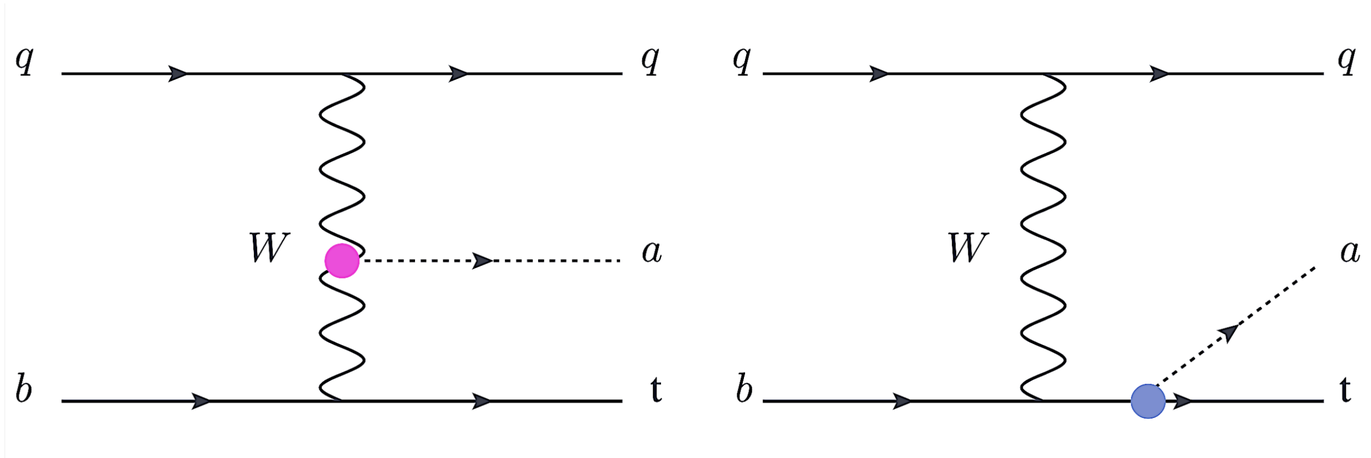

K.C., Chih-Ting, Priyanka, Ouseph 2404.14833

Interaction Lagrangian

$$\mathcal{L}_{\rm EW} \supset -\frac{a}{f_a}\left(C_{WW}W^i_{\mu\nu}\tilde{W}^{i\mu\nu} + C_{BB}B_{\mu\nu}\tilde{B}^{\mu\nu}\right),$$

$$\mathcal{L}_{at\bar{t}} = -iC_{a\phi}\frac{m_t a}{f_a}(\bar{t}\gamma^5 t).$$

$$\mathcal{L}_{\rm EW} \supset -\frac{1}{4}a\left(g_{a\gamma\gamma}F_{\mu\nu}\tilde{F}^{\mu\nu} + g_{a\gamma Z}F_{\mu\nu}\tilde{Z}^{\mu\nu} + g_{aZZ}Z_{\mu\nu}\tilde{Z}^{\mu\nu} + g_{aWW}W_{\mu\nu}\tilde{W}^{\mu\nu}\right),$$

- Consider: $pp \to qb \to tja$

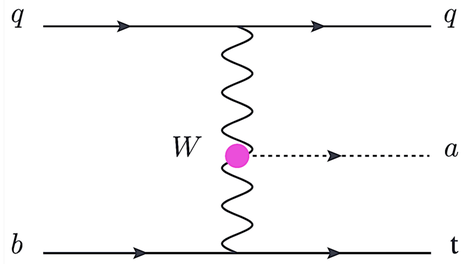

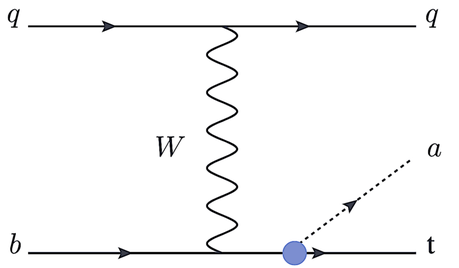

- $pp \to gq \to t\bar{b}ja$

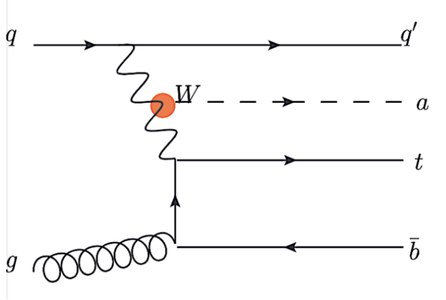

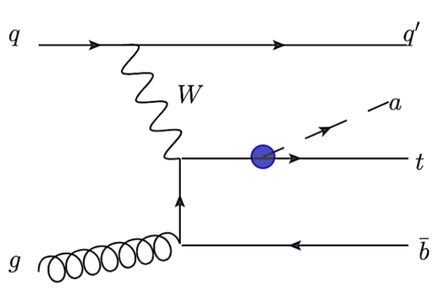

- $pp \to gb \to tWa$

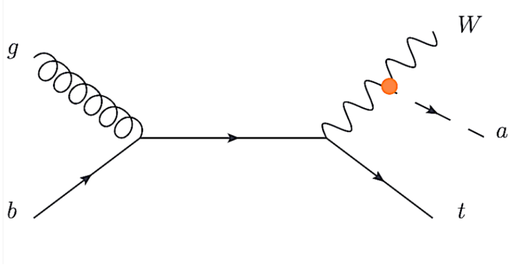

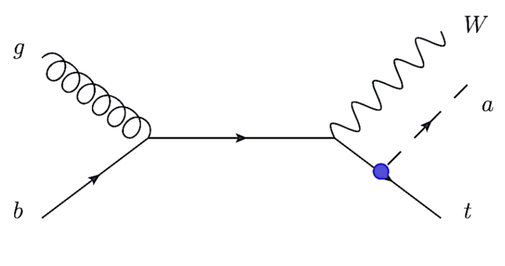

- $pp \to q\bar{q}' \to t\bar{b}a$

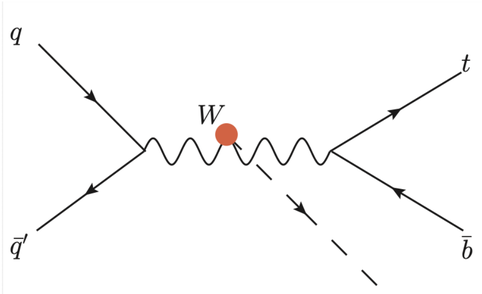

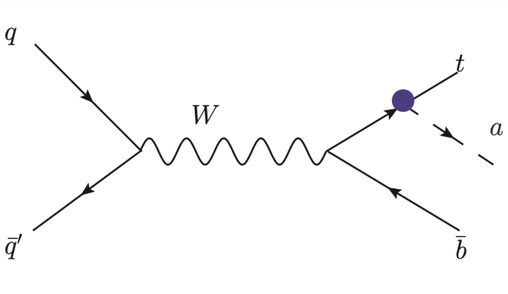

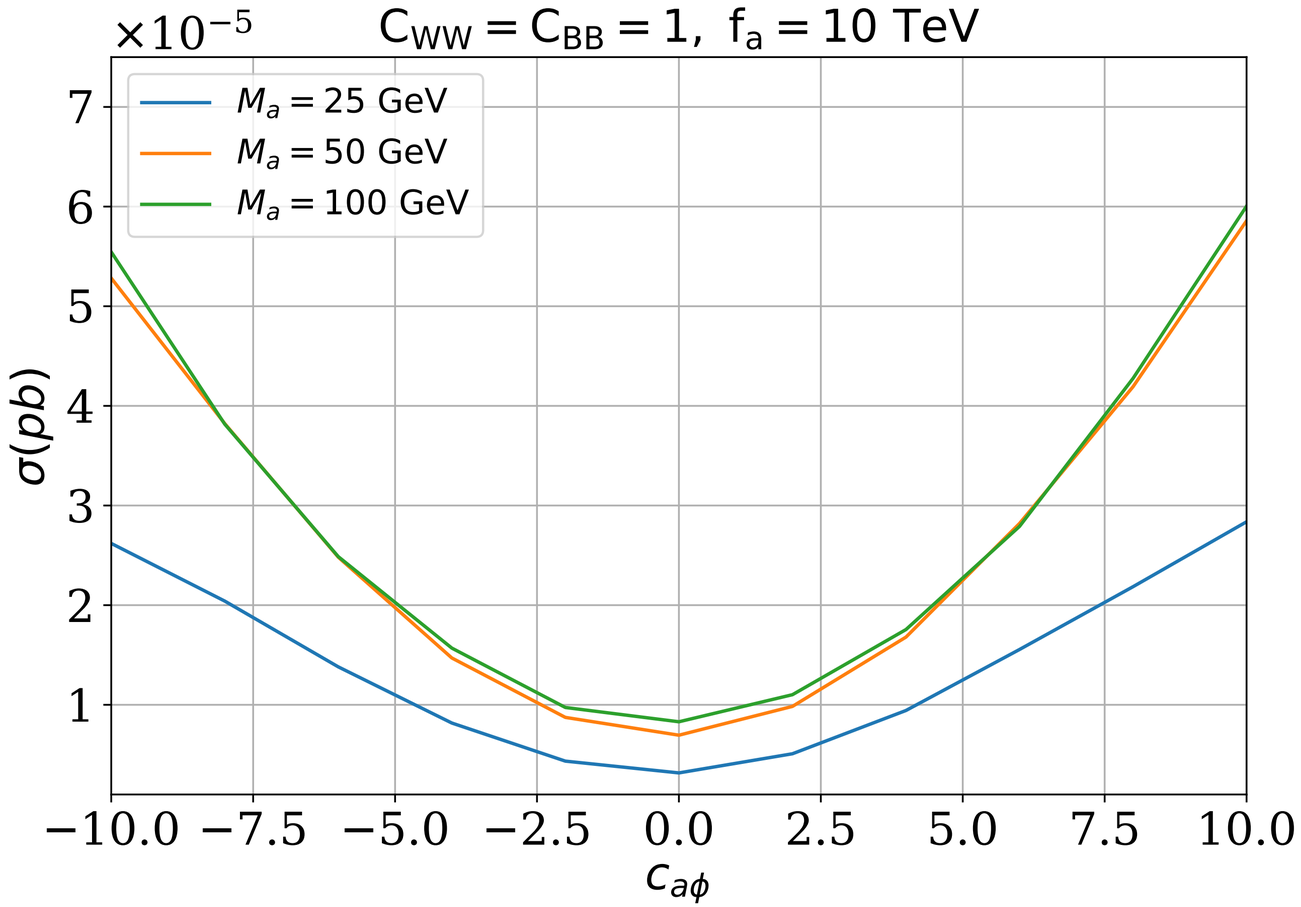

FIG. 2: Production cross sections for the signal process $pp \to j\ t\ a$ with $a \to \gamma\gamma$ and $t \to bW,\ W \to l\nu_l$ at the LHC ($\sqrt{s} = 14$ TeV) for $M_a = 25, 50, 100$ GeV. We fix the aW^+W^- coupling by setting $C_{WW} = C_{BB} = 1$ and $f_a = 10$ TeV. The $at\bar{t}$ coupling $C_{a\phi}$ varies from -10 to $+10$.

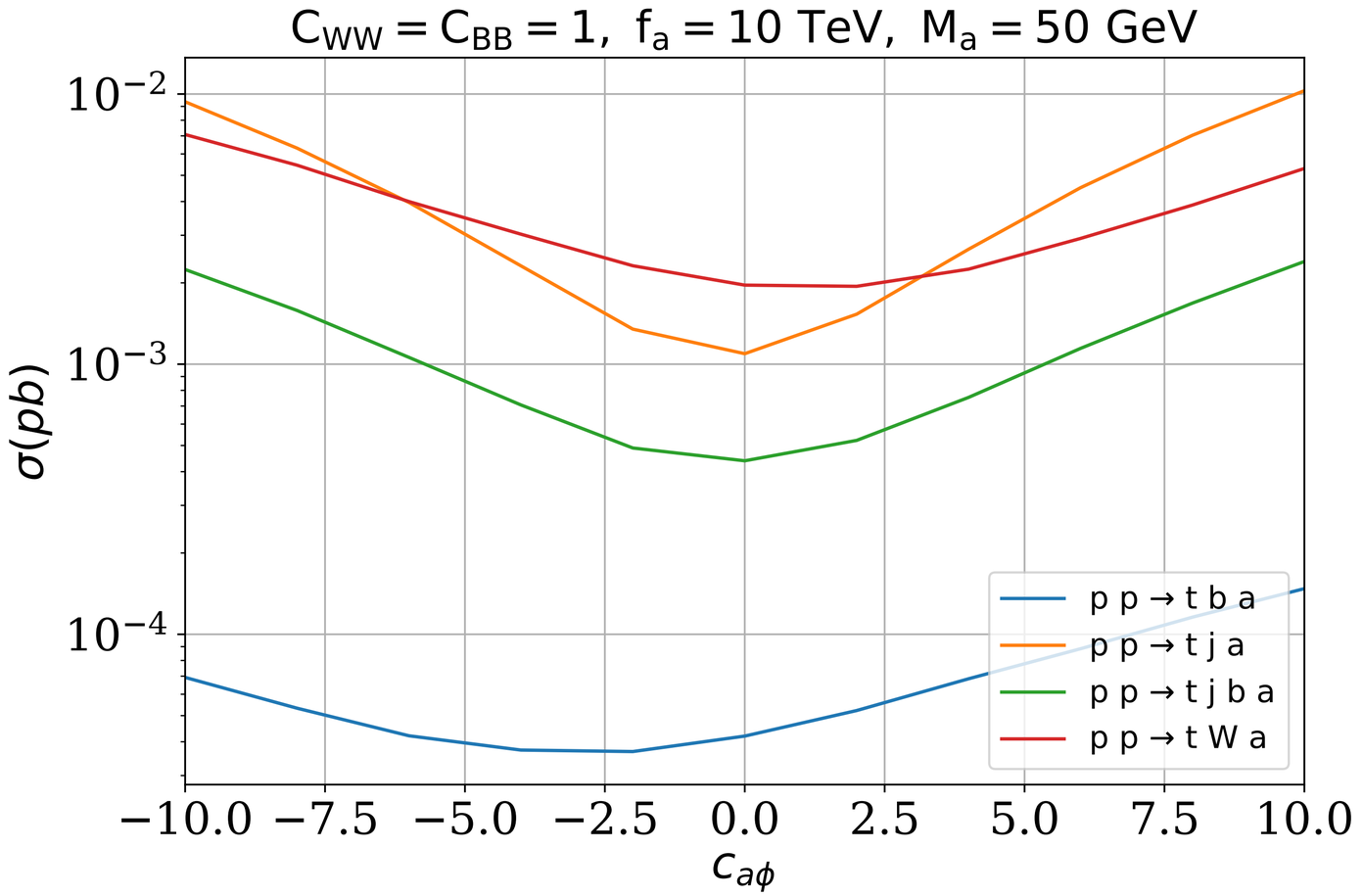

FIG. 6: Production cross sections for the signal processes $pp \to t\ j\ a$, $pp \to t\ j\ b\ a$, $pp \to t\ W\ a$, and $pp \to t\ b\ a$ at the LHC ($\sqrt{s} = 14$ TeV) for $M_a = 50$ GeV. We fix the ALP-gauge boson pair coupling by setting $C_{WW} = C_{BB} = 1$ and $f_a = 10$ TeV. The $at\bar{t}$ coupling $C_{a\phi}$ varies from -10 to $+10$.

Signal-Background analysis for $qb \to q'ta$

- Final state consists of $q'ta \to j(b\ell\nu)(\gamma\gamma)$.

  Benchmark: $f_a = 10\,\text{TeV},\ C_{WW} = C_{BB} = 1,\ C_{a\phi} = -10 \text{ to } 10$

- Backgrounds: (i) $pp \to tj\gamma\gamma$ (BG1), (ii) $pp \to Wjj\gamma\gamma$ (BG2)

- Signal and background event rates:

$$N_s, N_b = \sigma_{s,b} \times \frac{N_{\text{selected}}}{N_{\text{sim}}} \times \mathscr{L} \times (\eta_{b-tag} \text{ or } \eta_{j\to b})$$

- B-tagging efficiency: $\eta_{b-tag} = 0.75$, mis-tag efficiency: $\eta_{j\to b} = 0.01$

$M_a = 50$ GeV, $f_a = 10$ TeV, $C_{WW} = C_{BB} = 1$, $C_{a\phi} = 10$

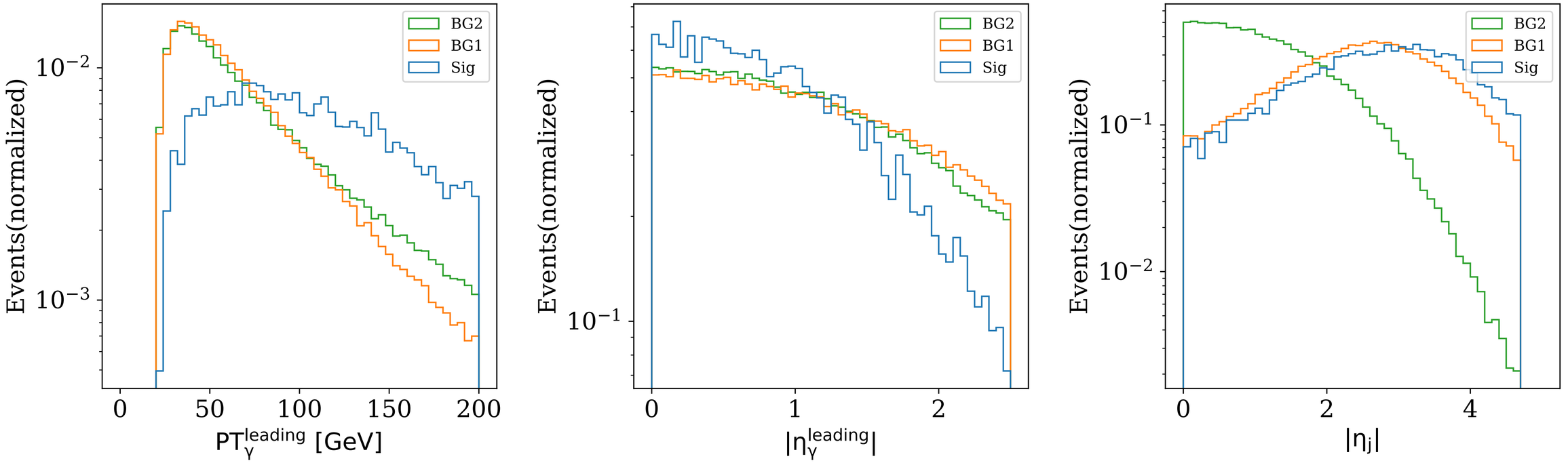

$$p_{T_\gamma}^{\text{leading}} > 60 \text{ GeV}, \quad |\eta_\gamma^{\text{leading}}| < 1.5, \quad 2.5 > |\eta_j| < 4.7$$

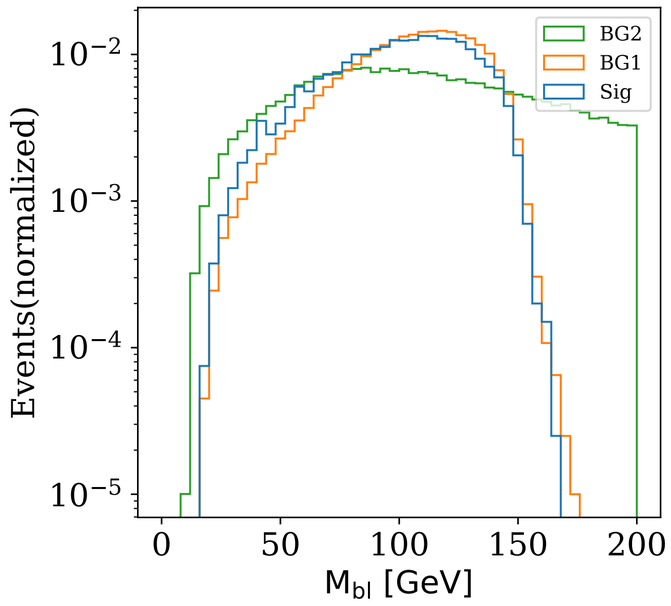

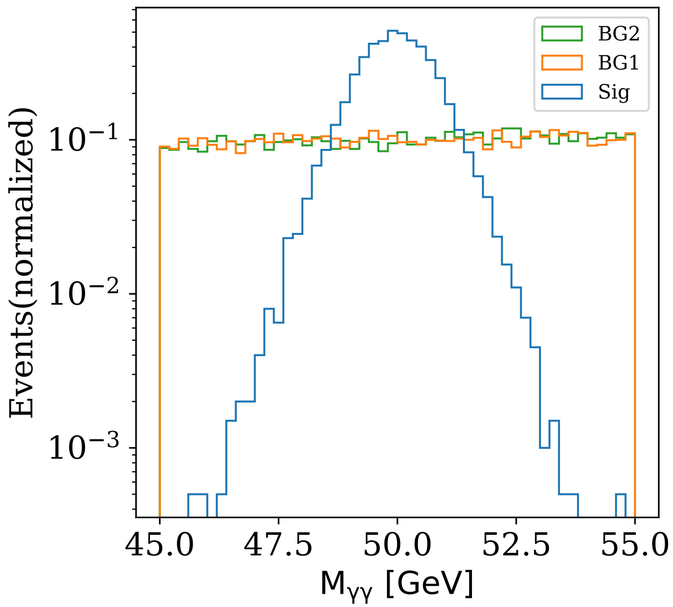

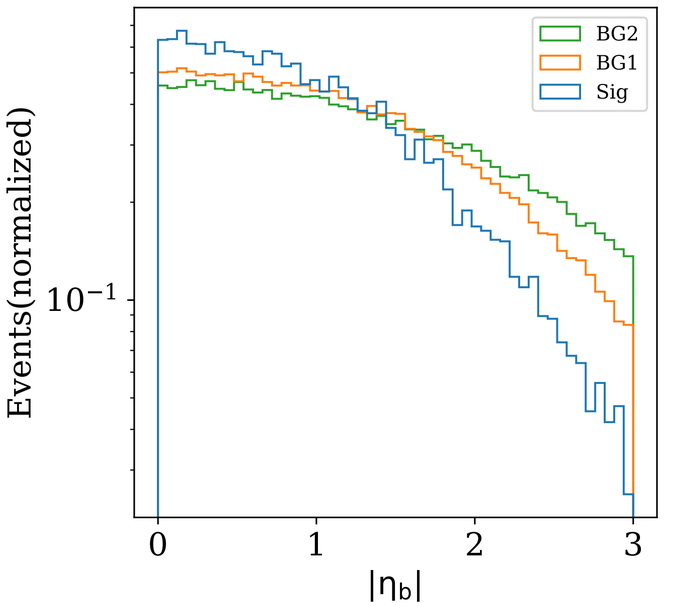

$$M_{bl} < 200 \text{ GeV}, \quad |\eta_b| < 1.5, \quad |M_{\gamma\gamma} - M_a| < 5 \text{ GeV}$$

Cut	**BG1**	**BG2**	**Signal**				
			$C_{a\phi} = -10$	$C_{a\phi} = -5$	$C_{a\phi} = 0$	$C_{a\phi} = 5$	$C_{a\phi} = 10$
NT	2318.39	307.86	120.56	43.26	15.73	49.69	131.68
$P_{T_\gamma}^{\text{leading}} > 60$ GeV	1181.01	170.03	99.22	36.80	14.83	42.53	109.11
$\lvert\eta_\gamma^{\text{leading}}\rvert < 1.5$	853.03	124.99	81.24	29.35	10.90	33.61	88.86
$2.5 < \lvert\eta_j\rvert < 4.7$	384.44	8.92	47.97	15.80	3.45	17.05	51.62
$M_{bl} < 200$ GeV	384.44	7.03	47.97	15.80	3.45	17.05	51.62
$\lvert\eta_b\rvert < 1.5$	266.20	4.68	37.94	12.38	2.56	13.47	40.46
45 GeV $< \text{M}_{\gamma\gamma} <$ 55 GeV	8.95	0.15	37.94	12.38	2.56	13.47	40.46

TABLE II: Cutflow table for the SM backgrounds (BG1: $p\ p \to t\ j\ \gamma\ \gamma$ and BG2: $p\ p \to W\ j\ j\ \gamma\ \gamma$) and the signal: $p\ p \to j\ t\ a$ with different $C_{a\phi}$ couplings. Here $M_a = 50$ GeV, $f_a = 10$ TeV, $C_{WW} = C_{BB} = 1$. The number of events are calculated by Eq. (10) and luminosity is set to $\mathcal{L} = 3000$ fb^{-1}.

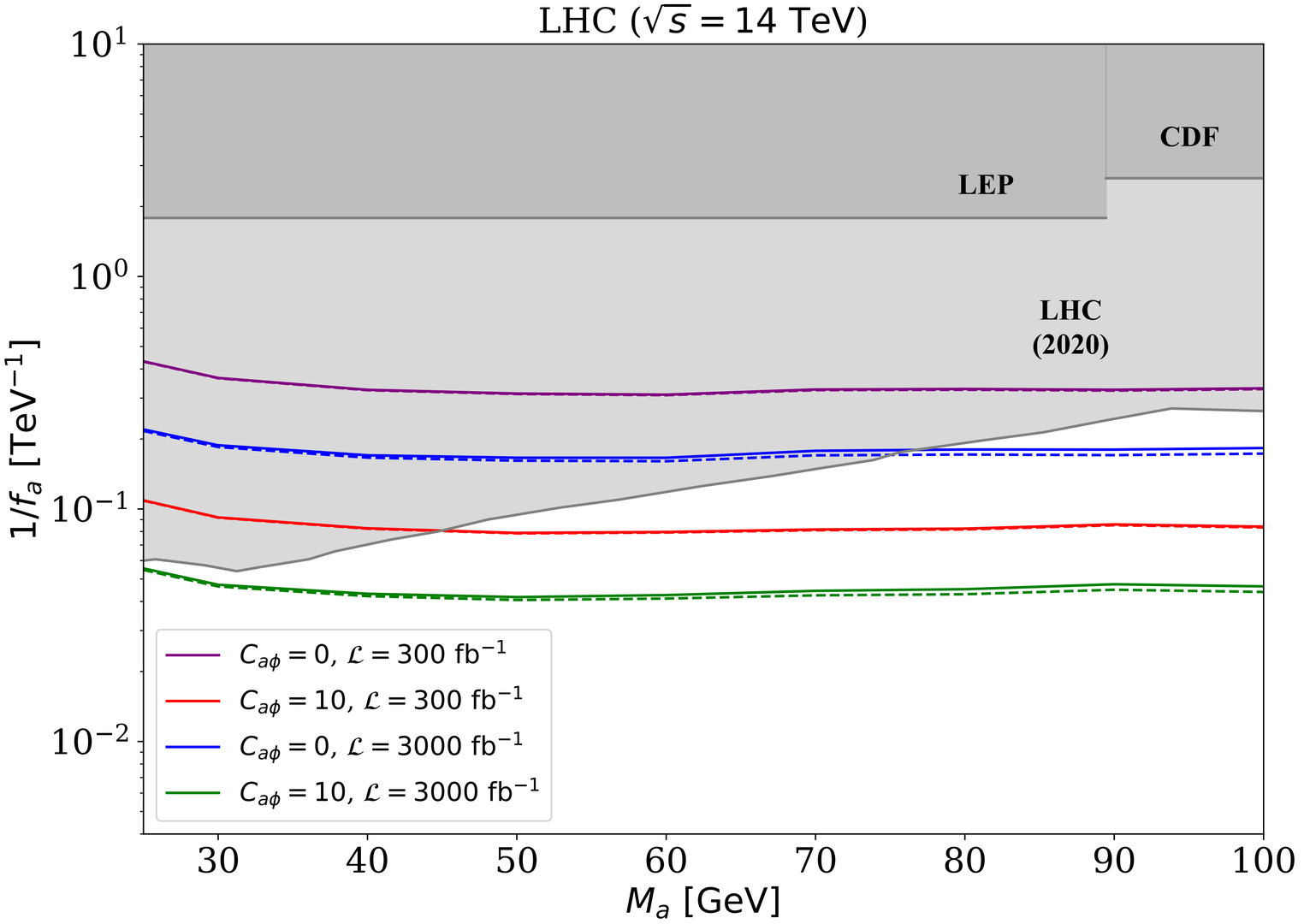

$$Z = \sqrt{2\left[(N_s+N_b)\ln\left(\frac{(N_s+N_b)(N_b+\sigma_B^2)}{N_b{}^2+(N_s+N_b)\sigma_B^2}\right)-\frac{N_b^2}{\sigma_B^2}\ln\left(1+\frac{\sigma_B^2 N_s}{N_b(N_b+\sigma_B^2)}\right)\right]},$$

95% CL calculated by Z=2.

Summary

- Interference effects between ALP-gauge ALP-top are present but mild.
- The channel can probe down to $1/f_a \sim 5 \times 10^{-2}\ \mathrm{TeV}^{-1}$

  for $m_a = 25 - 100\ \mathrm{GeV}$

Cut	**BG1**	**BG2**	**Signal**				
			$C_{a\phi} = -10$	$C_{a\phi} = -5$	$C_{a\phi} = 0$	$C_{a\phi} = 5$	$C_{a\phi} = 10$
NT	2318.39	307.86	59.17	24.68	7.12	27.53	63.69
$P_{T_\gamma}^{\text{leading}} > 60$ GeV	1181.01	170.03	41.28	17.96	6.04	20.45	45.44
$\lvert\eta_\gamma^{\text{leading}}\rvert < 1.5$	853.03	124.99	32.76	13.97	4.15	15.66	35.88
$2.5 < \lvert\eta_j\rvert < 4.7$	384.44	8.92	19.38	7.78	1.39	8.26	20.54
$M_{bl} < 200$ GeV	384.44	7.03	19.38	7.78	1.39	8.26	20.54
$\lvert\eta_b\rvert < 1.5$	266.20	4.68	14.85	5.93	1.00	6.28	15.69
20 GeV $< \text{M}_{\gamma\gamma} <$ 30 GeV	4.08	0.06	14.85	5.93	1.00	6.28	15.69

TABLE I: Cutflow table for the SM backgrounds (BG1: $p\ p \to t\ j\ \gamma\ \gamma$ and BG2: $p\ p \to W\ j\ j\ \gamma\ \gamma$), and the signal: $p\ p \to j\ t\ a$ with various $C_{a\phi}$ couplings. Here we set $M_a = 25$ GeV, $f_a = 10$ TeV, $C_{WW} = C_{BB} = 1$, and $C_{a\phi} = -10, -5, 0, 5, 10$ GeV. **NT** in the first row denotes the total number of events with basic cuts shown in Appendix A before further event selections. The number of events are calculated by Eq. (10) and integrated luminosity is set to $\mathcal{L} = 3000$ fb^{-1}. It is noteworthy that the number of events

Axion Dark Matter

Experimental hunt

- Strong motivation for current und upcoming axion DM experiments:

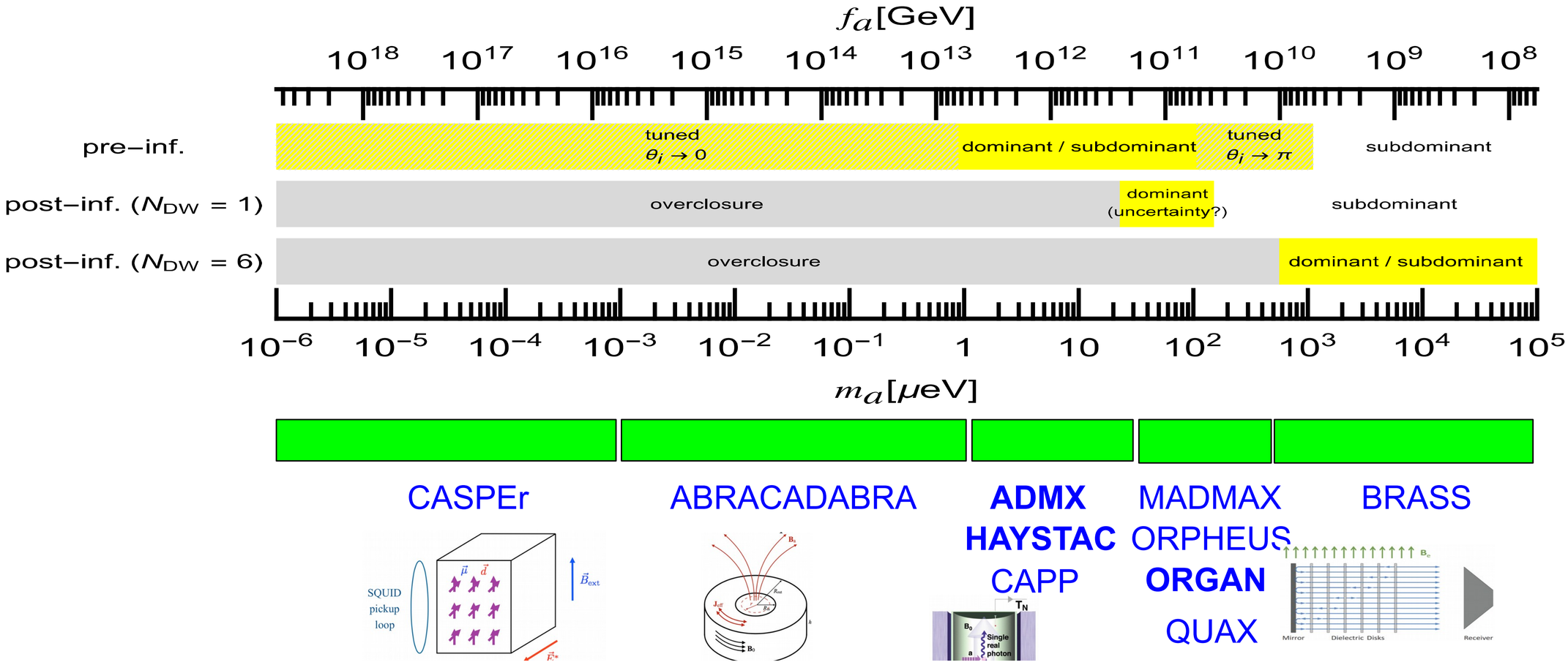

Cut	**BG1**	**BG2**	**Signal**				
			$C_{a\phi} = -10$	$C_{a\phi} = -5$	$C_{a\phi} = 0$	$C_{a\phi} = 5$	$C_{a\phi} = 10$
NT	2318.39	307.86	124.01	44.55	18.81	50.40	136.64
$P_{T_\gamma}^{\text{leading}} > 60$ GeV	1181.01	170.03	115.96	42.07	18.39	47.90	128.89
$\lvert\eta_\gamma^{\text{leading}}\rvert < 1.5$	853.03	124.99	97.00	34.28	14.13	38.80	106.93
$2.5 < \lvert\eta_j\rvert < 4.7$	384.44	8.92	58.41	17.88	4.16	19.29	62.29
$M_{bl} < 200$ GeV	384.44	7.03	58.41	17.88	4.16	19.29	62.29
$\lvert\eta_b\rvert < 1.5$	266.20	4.68	46.02	14.12	3.19	15.37	49.38
95 GeV $< \mathrm{M}_{\gamma\gamma} <$ 105 GeV	19.40	0.31	45.76	14.07	3.18	15.28	49.23

TABLE III: Cutflow table for the SM background (BG1: $p\ p \to t\ j\ \gamma\ \gamma$ and BG2: $p\ p \to W\ j\ j\ \gamma\ \gamma$) and the signal: $p\ p \to j\ t\ a$ with different $C_{a\phi}$ couplings. Here $M_a = 100$ GeV, $f_a = 10$ TeV, $C_{WW} = C_{BB} = 1$. The number of events are calculated by Eq. (10) and luminosity is set to $\mathcal{L} = 3000$ fb^{-1}.

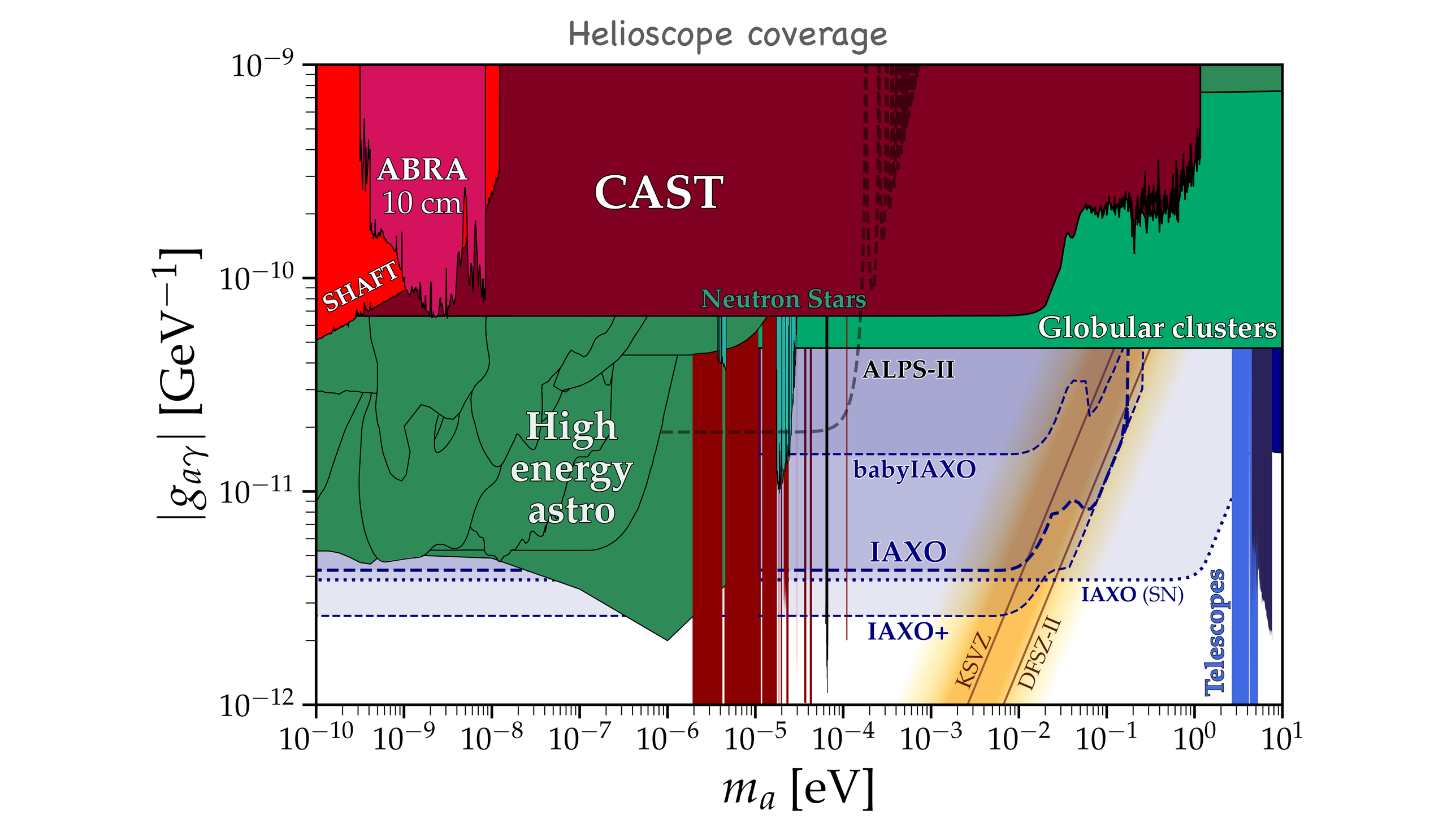
Helioscope coverage
ABRA
10 cm
SHAFT
CAST
Neutron Stars
Globular clusters
ALPS-II
High
energy
astro
babyIAXO
IAXO
IAXO (SN)
IAXO+
KSVZ
DFSZ-II
Telescopes
$|g_{a\gamma}|$ [GeV^{-1}]
m_a [eV]
10^{-9}
10^{-10}
10^{-11}
10^{-12}
10^{-10} 10^{-9} 10^{-8} 10^{-7} 10^{-6} 10^{-5} 10^{-4} 10^{-3} 10^{-2} 10^{-1} 10^{0} 10^{1}

Axion Dark Matter

- DM prediction: $\Omega_a h^2 \simeq \left(\frac{f_a}{9\times 10^{11}\ \mathrm{GeV}}\right)^{1.165} \theta_i^2 \simeq 0.12 \left(\frac{6\mu\mathrm{eV}}{m_a}\right)^{1.165} \theta_i^2$
- For $f_a > 10^9$ GeV, axion DM can be substantial and even 100%.
- A lot of experiments searching for axion DM: